

Research paper

Platelet factor 4 promotes rapid replication and propagation of Dengue and Japanese encephalitis viruses



Amrita Ojha ^{a,b}, Angika Bhasym ^{a,b,1}, Sriparna Mukherjee ^{c,1}, Gowtham K. Annarapu ^a, Teena Bhakuni ^a, Irshad Akbar ^c, Tulika Seth ^d, Naval K. Vikram ^d, Sudhanshu Vrati ^a, Anirban Basu ^c, Sankar Bhattacharyya ^e, Prasenjit Guchhait ^{a,*}

^a Disease Biology Laboratory, Regional Centre for Biotechnology, National Capital Region Biotech Science Cluster, Faridabad, India

^b Department of Biotechnology, Manipal Academy of Higher Education, Manipal, India

^c National Brain Research Centre, Manesar, India

^d All India Institute of Medical Sciences, New Delhi, India

^e Vaccine and Infectious Disease Research Centre, Translational Health Science and Technology Institute, National Capital Region Biotech Science Cluster, Faridabad, India

ARTICLE INFO

Article history:

Received 27 August 2018

Received in revised form 11 November 2018

Accepted 23 November 2018

Available online 5 December 2018

Keywords:

Platelet cytokine PF4

DV and JEV replication and propagation

Monocytes and microglia cells

ABSTRACT

Background: Activated platelets release cytokines/proteins including CXCL4 (PF4), CCL5 and fibrinopeptides, which regulate infection of several pathogenic viruses such as HIV, H1N1 and HCV in human. Since platelet activation is the hallmark of Dengue virus (DV) infection, we investigated the role of platelets in DV replication and also in a closely related Japanese Encephalitis virus (JEV).

Methods and findings: Microscopy and PCR analysis revealed a 4-fold increase in DV replication in primary monocytes or monocytic THP-1 cells *in vitro* upon incubation with either DV-activated platelets or supernatant from DV-activated platelets. The mass spectrometry based proteomic data from extra-nuclear fraction of above THP-1 lysate showed the crucial association of PF4 with enhanced DV replication. Our cytokine analysis and immunoblot assay showed significant inhibition of IFN- α production in monocytes *via* p38MAPK-STAT2-IRF9 axis. Blocking PF4 through antibodies or its receptor CXCR3 through inhibitor *i.e.* AMG487, significantly rescued production of IFN- α resulting in potent inhibition of DV replication in monocytes. Further, flow cytometry and ELISA data showed the direct correlation between elevated plasma PF4 with increased viral NS1 in circulating monocytes in febrile DV patients at day-3 of fever than day-9. Similarly, PF4 also showed direct effects in promoting the JEV replication in monocytes and microglia cells *in vitro*. The *in vitro* results were also validated in mice, where AMG487 treatment significantly improved the survival of JEV infected animals. Interpretation: Our study suggests that PF4-CXCR3-IFN axis is a potential target for developing treatment regimen against viral infections including JEV and DV.

© 2018 The Authors. Published by Elsevier B.V. This is an open access article under the CC BY-NC-ND license (<http://creativecommons.org/licenses/by-nc-nd/4.0/>).

1. Introduction

Platelet activation is a hallmark event in many viral infections including human immunodeficiency virus (HIV), hepatitis C virus (HCV), H1N1 influenza, Ebola and Dengue viruses (DV) [1–5]. The circulating platelets get activated either by the direct binding of viruses such as HIV-1, HCV and Dengue [3,5–7], or by the host inflammatory response including the cytokine and chemokine [8,9], and increase further risk of thrombocytopenia in patients. A recent study reported that the inhibition of platelet activation by an antagonist to platelet activation

factor (PAF) receptor rescued the event of thrombocytopenia in Dengue patients [10].

Activated platelets release several proteins and cytokines, which regulate the viral infections. The platelet factor 4 (PF4), also known as CXCL4, one of the abundant platelet cytokines, has been shown to be elevated in plasma of the Dengue patients [11]. PF4 in patient's plasma is described as the broad-spectrum inhibitor to HIV-1 infections [12]. Besides, studies also have shown PF4 as potent enhancer to HIV-1 replication in M-CSF-derived macrophages [13] and inducer to hepatitis-mediated liver fibrosis [14]. PF4 has been shown to be associated with H1N1 influenza infection. PF4 deletion resulted in diminished viral clearance from the lung and decrease lung inflammation during early infection but more severe lung pathology relative to wild-type mice during late infection of H1N1 [15]. Other platelet cytokines such as CCL5 and CCL3 are described as major suppressors to HIV-1 infections

* Corresponding author.

E-mail address: prasenjtit@rcb.res.in (P. Guchhait).

¹ Equal contribution.

Research in context

Evidence before this study

Viruses use host cells for replication and propagation. Although studies explain the mechanisms, but it is not clear yet, how the viral infections are rapidly elevated within 2–3 days after gaining entrance in the host. We have investigated the mechanism using closely related flaviviruses such as Dengue virus (DV) and Japanese Encephalitis virus (JEV).

Added value of this study

We describe that the host protein platelet factor 4 (PF4) promoted replication and propagation of both DV and JEV in monocytes. In presence of either the supernatant of activated-platelets or rhPF4, the synthesis of new virions for both DV and JEV was increased significantly in monocytes or microglia cells *in vitro*. Besides, PF4 decreased the IFN- α secretion in monocytes. Our data from dengue patients and JEV infected mice also confirmed direct correlation between elevated plasma PF4 and increased viral replication. Further the blocking of PF4 receptor CXCR3 with AMG487 treatment significantly decreased JEV infection while enhancing survival of infected mice.

Implication

Therefore, our study suggests that PF4-CXCR3-IFN axis is a potential target for developing treatment against viral infections including DV and JEV. Antagonists to CXCR3 including AMG487 can be useful for treatment against JEV and DV, and may be for other viruses.

[16]. The CCL5 is reported as inhibitor to influenza A [17] and HCV [18]. Likewise, other platelets-derived proteins and peptides including β -defensins, serotonin, PD3 and PD4, and thymosin β 4, CXCL7, cleaved products of fibrinopeptide A/B and thrombospondins are reported to be playing important role in neutralizing viral infections [19–21].

Several studies including our recent work describe that upon activation by DV platelets are engulfed rapidly and removed from circulation by the phagocytic cells including monocytes and macrophages [5,22,23]. On the other hand, the viruses including DV use these host cells as the incubators for replication and rapid propagation [24,25]. Monocytes are the most abundant blood mononuclear phagocytes and one of the main cell targets of DV. Half of the DV-antigen positive monocytes contained replicating viruses [26]. A recent report suggests that despite the lack of transcriptional machinery, platelets are able to provide the cellular platform for replication and propagation of DV *in vitro* as well as *in vivo* [6].

Because viruses replicate within the cell, they are vulnerable to any intracellular alteration caused by host response to infection. The inflammatory mediators including TNF- α and IL-1 β and interferons alter the intracellular environment and affect viral replication [27]. In response to viral infections the host immune cells induce the interferon secretion that inhibits further the viral replication in host cells and also abrogates the entry of virus to other cells [28,29]. Although the interaction between virus and host immune response is well reported, but several queries remain unexplained. It is not clearly understood - how viruses replicate and propagate rapidly in host cells specifically inside phagocytic immune cells such as monocytes? Dengue virus propagates rapidly within 3 days of gaining entrance in the host through mosquito bite. Since it is well reported that maximum platelet activation [5,6] and viral replication [26] occur parallelly between 3 and 4 days of infection, we investigated whether the DV replication and propagation in host

cells including monocytes are different when these phagocytic cells interact with DV-activated platelets in circulation of a patient.

Our study described the significantly enhanced replication of DV in monocytes *in vitro* in presence of a relevant concentration of PF4 observed in plasma of Dengue patients [11]. PF4 increased p38 MAPK activation and down regulated STAT-2 – IRF-9 signaling to decrease the synthesis and secretion of IFN- α and other inflammatory cytokines such as TNF α , IL-1 β and IL-6 in monocytes. Blocking PF4 through antibodies or its receptor CXCR3 through inhibitor *i.e.* AMG487, significantly rescued the cytokine production and abrogated DV replication in monocytes. To investigate further whether the above mechanism exists in other viruses including Japanese Encephalitis virus (JEV), a close relative of DV, our study described the similar elevation in viral replication in monocytes as well as microglia cells mediated by PF4 *in vitro*, while simultaneously inhibiting the IFN- α signaling in these infected cells. Blocking of CXCR3 through inhibitor AMG487 significantly rescued the mice from JEV infections and significantly enhanced their survival.

2. Methods

2.1. Materials

The antibodies for phospho and non-phospho STAT-2, NF κ B (p65/66) and p38, and IRF-9 were purchased from Cell Signaling, Beverly, USA; dsRNA (J2: English and Scientific consulting Bt., Hungary); DV NS1, PF4 and LAMP-1 (Abcam, Cambridge, USA); β -Actin (Thermo Scientific, Rockford, USA), goat anti-rabbit and goat anti-mouse HRP conjugated antibody (Pierce, Rockford, USA); anti-human CD14-FITC, anti-human CD41a-PE and antibodies (BD Biosciences); anti-mouse AF488, anti-rabbit AF594 (Thermo Scientific, Rockford, USA). ELISA kits for human PF4 and mouse PF4 (R&D Systems, USA), Dengue NS1 (PanBio, Brisbane, Australia). Annexin V- FITC and recombinant human PF4 (R&D Systems, USA); human fibrinogen and thrombospondin (R&D Systems, USA) and AMG487 (Tocris Biosciences, USA).

2.2. Human subjects

The ethics approval was obtained from the Institutional Ethics Committee of Regional Centre for Biotechnology (RCB), Faridabad and All India Institute of Medical Sciences (AIIMS), New Delhi for the collection of peripheral blood from dengue patients. Informed consent was provided according to the recommendations of the declaration of Helsinki. 6 mL blood sample was collected in citrate anticoagulant from 20 dengue patients at day-3 of fever when they got admission at AIIMS after detection of low platelet counts, plasma NS1 positivity and high fever. Further the blood sample was collected from those patients at day-5 and day-9. The subtypes of DV (DV 1–4) or the types of infections such as primary or secondary were not determined. The platelet counts and other clinical information is mentioned in Table-S1. Blood sample was collected from healthy individuals ($n = 10$) without any recent history of Dengue or any such infection. Plasma and peripheral blood mononuclear cells (PBMCs) were stored for further assays. An estimated 30 mL blood was collected from healthy individuals ($n = 10$) in acid citrate-dextrose (ACD) anticoagulant for isolation of PBMCs and monocytes for *in vitro* experiments.

2.3. Mice and infection study

All experiments were performed after obtaining approval from the Institutional Animal Ethics Committee of the National Brain Research Centre (Approval number: NBRC/IAEC/2016/116) within the framework of the Committee for the Purpose of Control and Supervision of Experiments on Animals (CPCSEA), Government of India. 10-day-old BALB/c mice pups of either sex were used for three experiments. In experiment-1, mice were injected with either AMG487 [(i.p. injection)

AMG487 dissolved in ethanol at 20 mg/mL and further diluted in phosphate-buffered saline (PBS) containing 10% Tween-80 to final concentration 4 mg/mL or vehicle [PBS containing 10% Tween-80] twice daily starting 12 h before the JEV injection [3×10^5 plaque-forming units (PFU) of Japanese Encephalitis virus (JEV) GP78 strain] till day 3 and sacrificed at day 4, ($n = 12$). In experiment-2, above treatment was continued till day 5 and sacrificed at day 6, ($n = 8$). In experiment-3, mice were treated till day 5 and allowed for survival, ($n = 15$). The detail experimental procedure is shown in Fig. 6A using schematic. The animals were sacrificed and the brains were excised and stored at -80°C for quantifying JEV infection.

2.4. Cells and viruses

The human monocytic cells THP-1 and monkey kidney cell line Vero (ATCC, USA), and murine microglial cell line BV2 (Anirban Basu's Laboratory, NBRC, India) were cultured at 37°C under 10% CO_2 in either RPMI along with 10% heat-inactivated fetal bovine serum (FBS, Gibco Invitrogen, USA) or DMEM with FBS, and 100 U penicillin/streptomycin. The cells were used for performing various experiments including infection assays as mentioned below. The viruses such as Dengue virus subtype-2 (DV2) NGC strain and JEV GP78 strain were used for following experiments at MOI of 3 and 5 respectively. Detail about both viruses is mentioned in our previous work [5].

2.5. Virus preparation

DV2 NGC strain and JEV GP78 strain were expanded in C6/36 cells cultured in L15 media supplemented with 10% FBS and standard concentrations of penicillin-streptomycin-glutamine. Cell supernatant was purified through 100 kDa cut-off membrane before use. Briefly, cells were infected using DV2/JEV inoculum diluted in L15 supplemented with 2% FBS for 2 h at 37°C , 5% CO_2 under continuous gentle rocking. At the end of infection the inoculum was discarded and complete L15 media overlaid on the cells. The infected cells were incubated at 37°C under 5% CO_2 for 5 days and 3 days for DV2 and JEV respectively. Subsequently the supernatant was collected and clarified by centrifugation at 1000 RPM for 10 min. The cell supernatant was aliquoted and stored at -80°C for further use. The amounts of infectious particles were expressed as focus forming units (FFU)/mL and titrated in Vero cells.

2.6. Washed platelet preparation

Platelet-rich plasma (PRP) obtained from the healthy individuals was centrifuged and the platelets were resuspended in calcium-free Tyrode buffer, 0.1% BSA, pH 6.5 and, gel-filtered on a column of Sepharose 2B (Sigma-Aldrich, St. Louis, USA) equilibrated in calcium-free Tyrode buffer, pH 7.2 as mentioned in our previous work [5].

2.7. Monocyte isolation, culture and treatment

The PBMCs were isolated from whole blood by density gradient centrifugation using Lymphoprep [30]. PBMCs were incubated with CD14^+ micro-bead (Miltenyibiotec, Germany) for 45 min at 4°C and monocytes were isolated through MACS column *via* positive selection. CD14^+ monocytes were seeded (1×10^5 cells/well) in 12-well cell plates (Corning, NY, USA), in RPMI-1640 medium (Sigma Aldrich, St. Louis, USA) supplemented with 10% (v/v) FBS, 100 U/mL penicillin, and 100 $\mu\text{g}/\text{mL}$ streptomycin for 2 h at 37°C in 5% CO_2 incubator, to allow monocytes to adhere to the plastic plate. Supernatant containing non-adherent cells was removed and the adherent monocytes 1×10^5 were washed and incubated with [1] 3×10^7 PFU DV2 (MOI-3), [2] DV-activated platelets (DV-activated platelets were prepared where platelets 1×10^7 were incubated with 3×10^7 PFU DV2 for 30 min at 37°C with mild rotation, and whole DV-platelet mixture was added to wells containing monocytes), and [3] untreated or resting platelets

(1×10^7). In experimental wells, the rPF4 (25, 50, 100 and 250 ng/mL) along with either anti-PF4 antibody (300 and 500 ng/mL) or CXCR3 antagonist AMG487 (2.5 μM) were added to monocytes. After 2 h, monocytes were washed with PBS to remove unbound virus or platelets before microscopy or other assays. Similarly the monocytic THP-1 cells treated as mentioned above and processed for assays. In another experiment, primary monocytes or mouse microglia cells were infected with 3×10^7 PFU JEV (MOI-3) in presence of PF4 with and without anti-PF4 or AMG487 and processed for assays as mentioned above for DV. After the experiments, the adherent monocytes were removed by incubating in ice-cold 10 mM EDTA in PBS solution for 10 min and utilized for further downstream processing using microscopy staining, qPCR, flow cytometry and protein immunoblot analysis.

2.8. Focus forming assay

Vero cells were incubated with serially diluted virus samples (collected from cell culture supernatants from monocytes mentioned above in section 2.7) for 2 h and the inoculum was discarded. These cells were subsequently incubated in complete growth media for 48 h and fixed using 2% PFA and permeabilized using phosphate-buffered saline (PBS) supplemented with 0.1% Triton-X-100. The infected cells were visualized in a fluorescence microscope after immune-staining using anti-flavivirus specific 4G2 primary antibody and Alexa-488 conjugated anti-mouse secondary antibody and estimated as focus forming units (FFU). Similarly, the infectious titre was calculated for JEV from the brain lysates of mice infected with JEV with/without AMG487 treatment. The FFU assay was performed as mentioned above.

2.9. Confocal microscopy and analysis

Monocytes, THP-1 cells or microglia cells from above treatment as mentioned above in section 2.7, were fixed in 4% paraformaldehyde and permeabilized using 0.1% Triton X-100 or 0.4% Tween-20 for 20 min at room temperature (RT). After blocking with 2% BSA for 1 h at RT cells were labeled with primary antibodies followed by Alexa 488/568/647 conjugated secondary antibody. Cells were mounted using ProLong Gold anti-fade reagent with DAPI. Images were captured using a Leica Confocal DMI 6000 TCS-SP8 microscope (Leica Microsystems, Wetzlar, Germany) at $63\times$ oil immersion objective (NA 1.4) Plan Apo objectives and quantified as mentioned [5]. Imaging was performed using Z-stacks at 0.20 μm per slice by sequential scanning and Image J Fiji software was used to generate cross-sectional and maximum intensity projection images. Briefly, region of interest (ROI) was drawn and integrated density of the maximum intensity projection image of fluorophore was measured using Image J Fiji software as mentioned [31]. Similarly, background integrated density was measured from area without fluorescence. The total cell fluorescence intensity was corrected by deducing background fluorescence from each cells integrated density. Likewise, corrected total cell fluorescence intensity was calculated from at least 25 cells in each set per experiment and data represented as mean and standard error of mean from at least 3 independent experiments.

2.10. Quantitative real time PCR (qRT-PCR)

Dengue viral RNA was isolated from primary monocytes or THP-1 cells from above treatment (section 2.7) using Ambion TRIzol Reagent (Thermo Fisher Scientific). The RNA (2 μg) was reverse transcribed using primer from Super Script IV First-Strand Synthesis System (Invitrogen, Thermo Fisher Scientific). The cDNA (1.6 μL) of each sample was subjected to qPCR using forward primer 5' -GARAGACCAGAGA TCCTGCTGTCT-3' and reverse primer 5' -ACCATTCCATTTCTGGCGTT-3' in TaqMan universal PCR master mix (Applied Biosystems) using Applied Biosystems 7500 real-time PCR system and data were analyzed as mentioned [5].

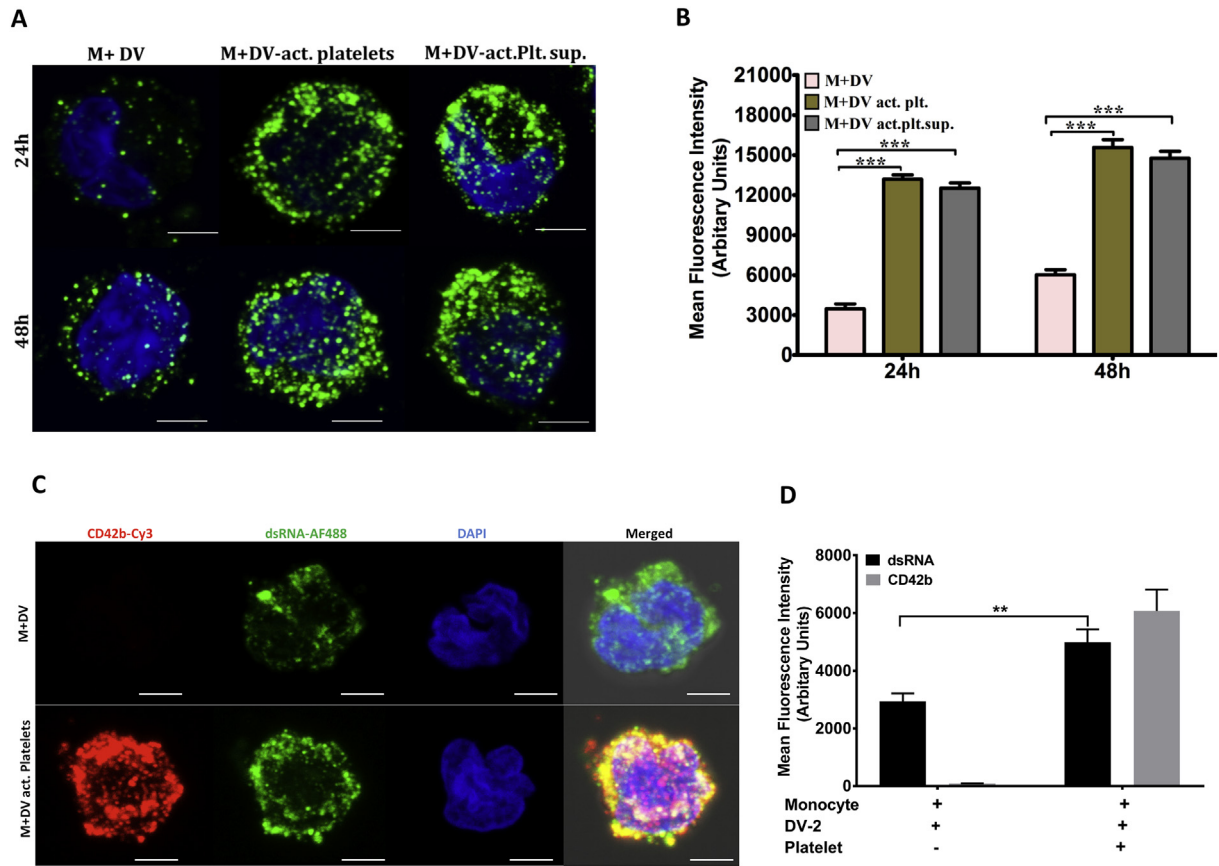


Fig. 1. Platelet or platelet supernatant increases replication and propagation of DV2 in monocytes *in vitro*. (A) Quantification of dsRNA. Primary monocytes isolated from peripheral blood of healthy individuals were incubated with DV2 or DV2-activated platelets (detail treatment is mentioned in section 2.7) Monocytes were stained for intracellular dsRNA (green) and nucleus (DAPI, blue). (B) The mean fluorescence intensity (MFI) for dsRNA was quantified (detail quantification method is mentioned in section 2.9) from 25 images from each above experiment (Fig. 1A) in triplicate and represented as mean \pm SEM. One-Way ANOVA with multiple comparison test was used, $***p < 0.0001$. (C) A similar experiment (as in Fig. 1A) showed colocalization of platelets (red) and dsRNA (green) in monocyte at 24 h. (D) MFI of platelet and dsRNA was quantified, $**p < 0.001$. (E) Quantification of viral genome. DV2 genome copies were measured using qPCR from the monocytes pellet from above experimental groups (as in Fig. 1A) at 2, 24, 48, 72 and 96 h. Data are mean \pm SEM and paired *t*-test was used, $*p = 0.0047$, $*p = 0.0008$, $**p = 0.0003$, $***p = 0.0002$. (F) Quantification of viral NS1. Monocytes were incubated with various numbers of platelets and same MOI of DV2 (detail mentioned in section 2.7). After 24 h, monocytes were stained for intracellular NS1 (FITC) and platelet CD41 (PE) and analyzed by flow cytometry. The NS1⁺CD41⁺ monocytes (%) were measured using paired *t*-test, $*p = 0.0201$, $**p = 0.0082$. (G) As mentioned in Fig. 1F the MFI of NS1 and CD41 was analyzed and paired *t*-test was used, $*p = 0.0353$, $**p = 0.0082$, $***p < 0.001$, ns = non-significant. Gating strategy is mentioned in Fig. S2. (H) Infection assay. Supernatant from above experiments where monocytes were either incubated with only-DV2 or DV2-activated platelets was used to infect Vero cells. The focus-forming unit (FFU) per ml of supernatant was calculated as \log_{10} (FFU/ml) was plotted against each time point. Data were analyzed using paired *t*-test, $**p = 0.0040$, $***p = 0.0009$. Bars ~ 5 μ m in all images in this Figure as well as other Figures.

2.11. JEV viral load detection from mice

RNA was extracted from tissue isolated from SVZ (sub ventricular zone) region of mouse brain using Trizol (Sigma Aldrich, USA) followed by chloroform and isopropanol treatment. The cDNA was synthesized from the isolated RNA using advantage RT-PCR Kit (Clontech, Mountain View, USA). The conditions for qPCR reactions was performed using JEV GP78 forward TTGACAATCATGGCAAACG and reverse CCCAACTTGCCTGAATAA primers, and normalized with mouse GAPDH by $\Delta\Delta$ CT method and are depicted as fold change over mock-infected control as mentioned [32].

2.12. Mass spectrometry methodology and analysis

The detail of this section 2.11 is mentioned in suppl. information.

2.13. Experimental design

The monocytic THP-1 cells were cultured with DV (THP1 + DV) or DV-activated platelets (THP1 + DV + PLT) and untreated platelets (THP1 + PLT) for 2 and 24 h as mentioned in above in section 2.7.

2.14. Cell fractionation using sucrose gradient ultracentrifugation

Cell pellet collected in protease inhibitor cocktail were homogenized using Dounce homogenization. The nuclear fraction was removed by centrifugation at 500 g for 10 min. The resulting post-nuclear supernatant (750 μ l) was fractionated using discontinuous sucrose gradient as mentioned [33]. Fractions were collected and separated on SDS-PAGE.

2.15. Sample preparation for mass spectrometry

The post-nuclear fractions rich in amphisomes and microsomes from THP-1 cell lysate from above experiments were processed for proteome analysis. The fractions were lysed and concentrated using Amicon® Ultra centrifugal filters with MWCO of 10 kDa. After gel purification proteins were trypsinized at 1:20 (p/p) enzyme (Trypsin Gold from Promega, USA)/substrate ratio for 18 h at 37 °C. 50 μ g of the initial digests were desalted using C18 resin (Applied Biosystems), packaged in micropipette tips (Millipore, Bedford, USA) and equilibrated in 1% formic acid. The peptides were eluted with formic acid (0.1%) containing acetonitrile (70%) and further dried using vacuum centrifuge.

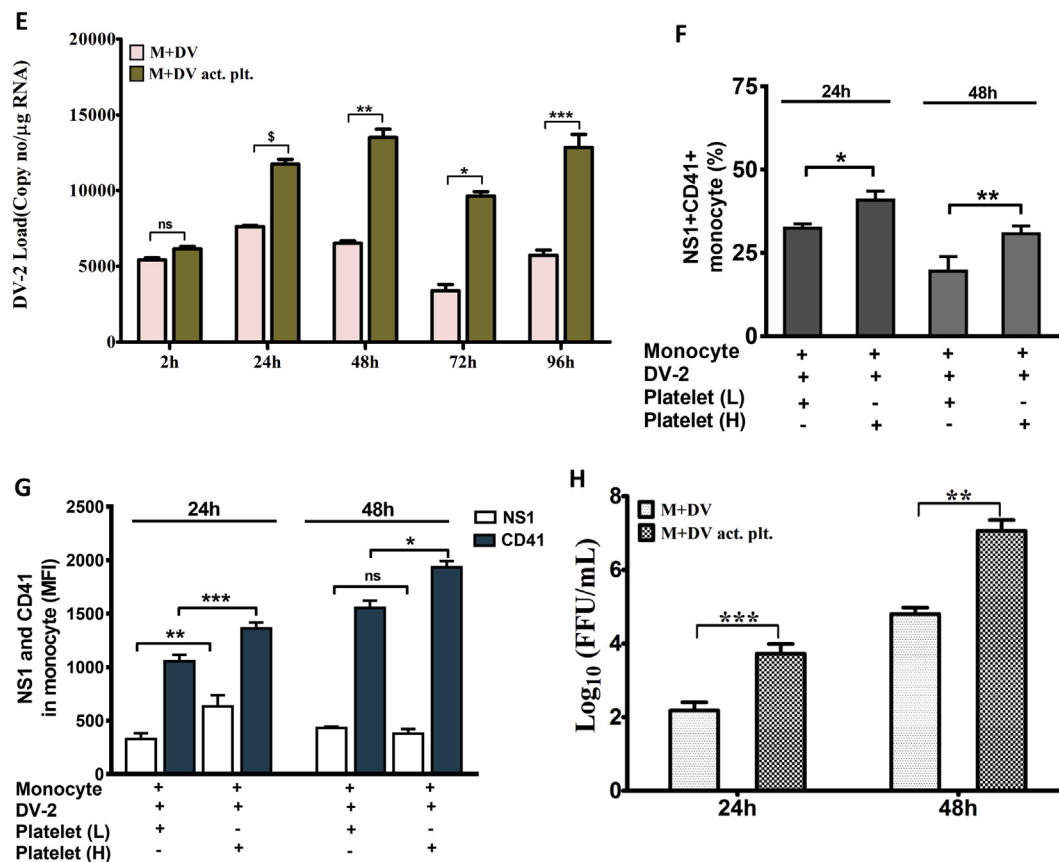


Fig. 1 (continued).

2.16. LC-MS/MS analysis

LC-MS/MS analysis was carried out as described previously [34]. Briefly, the desalted pooled sample was then lyophilized and reconstituted with 98% water, 2% acetonitrile with 0.1% formic acid. Peptides were separated using nanoLC Ultra in Trap Elute configuration. The samples were loaded on a trap column of 350 μm × 0.5 cm (ChromXP C18-CL, 3 μm) and eluted on a 150–0.1 mm column (Chromolith CapRod, RP-18e). MS analysis was performed in information-dependent mode using a 5600 TripleTOF analyzer (AB SCIEX).

2.17. Peptide and protein identification

Peptide identification and quantification was carried out on the ProteinPilot 4.5 software Revision1656 (AB SCIEX, 2012) using the Paragon™ algorithm and the integrated false discovery rate (FDR) analysis function and peptide shaker search engine. The search was conducted using SearchGUI version 1.16.18 [35]. Protein identification was conducted against a concatenated target/decoy [36] version of the *Homo sapiens* (20,316, >99.9%), *Susscrofa* (1, <0.1%) complement of the UniProtKB [37]. The decoy sequences were created from the target sequences in SearchGUI. The identification settings were as follows: Trypsin, Specific, with a maximum of 2 missed cleavages 50.0 ppm as MS1 and 0.02 Da as MS2 tolerances; fixed modifications: Carbamidomethylation of C (+57.021464 Da), variable modifications: Oxidation of M (+15.994915 Da), fixed modifications during refinement procedure: Carbamidomethylation of C (+57.021464 Da), variable modifications during refinement procedure: Acetylation of protein N-term (+42.010565 Da).

2.18. Quantification

Around 259, 487 and 501 proteins (mentioned in suppl. Table-S2) were identified in respective group *i.e.* THP1 + DV, THP1 + DV + PLT and THP1 + PLT. Out of the total identified proteins in each group, the exclusive proteins (including platelet and viral proteins) were identified in THP1 + DV + PLT and THP1 + DV data sets at 24 h (when the viral replication was significantly high) by eliminating the common proteins at 2 h (when almost no viral replication was detected) in respective groups using Venny 2.1.0. Simultaneously, the platelet proteins were segregated using PlateletWeb database (<http://plateletweb.bioapps.biozentrum.uni-wuerzburg.de/plateletweb.php>) from the total proteins. These unique proteins were further used to build a protein-protein interaction (PPI) network to identify the gene ontology (GO) of biological processes using IPA (Ingenuity Systems®, www.ingenuity.com) setting experimental evidence as a criterion. The networks associated with viral replication and viral infection was selected for further analysis based on the *p* value (threshold *p* value < 3 × 10⁻¹⁵). We found that some of platelet proteins, which were abundant in cell lysate at 24 h, were associated with viral replication and infection networks. The proteins from above networks were grouped and further analyzed for differential expression using normalized spectral count method (NSAF score calculation). NSAF values for each protein were calculated using already reported algorithm [38]. The above peptides and proteins were inferred from the spectrum identification results using PeptideShaker version 1.16.23 [39]. Spectrum counting abundance indexes were estimated using the Normalized Spectrum Abundance Factor [40], adapted for better handling of protein inference issues and peptide detectability. NSAF ratios of ≥1.2 and ≤0.5 were considered significant. Gene ontology analysis showed maximum association of platelet factor 4 (PF4) with viral replication and viral infection

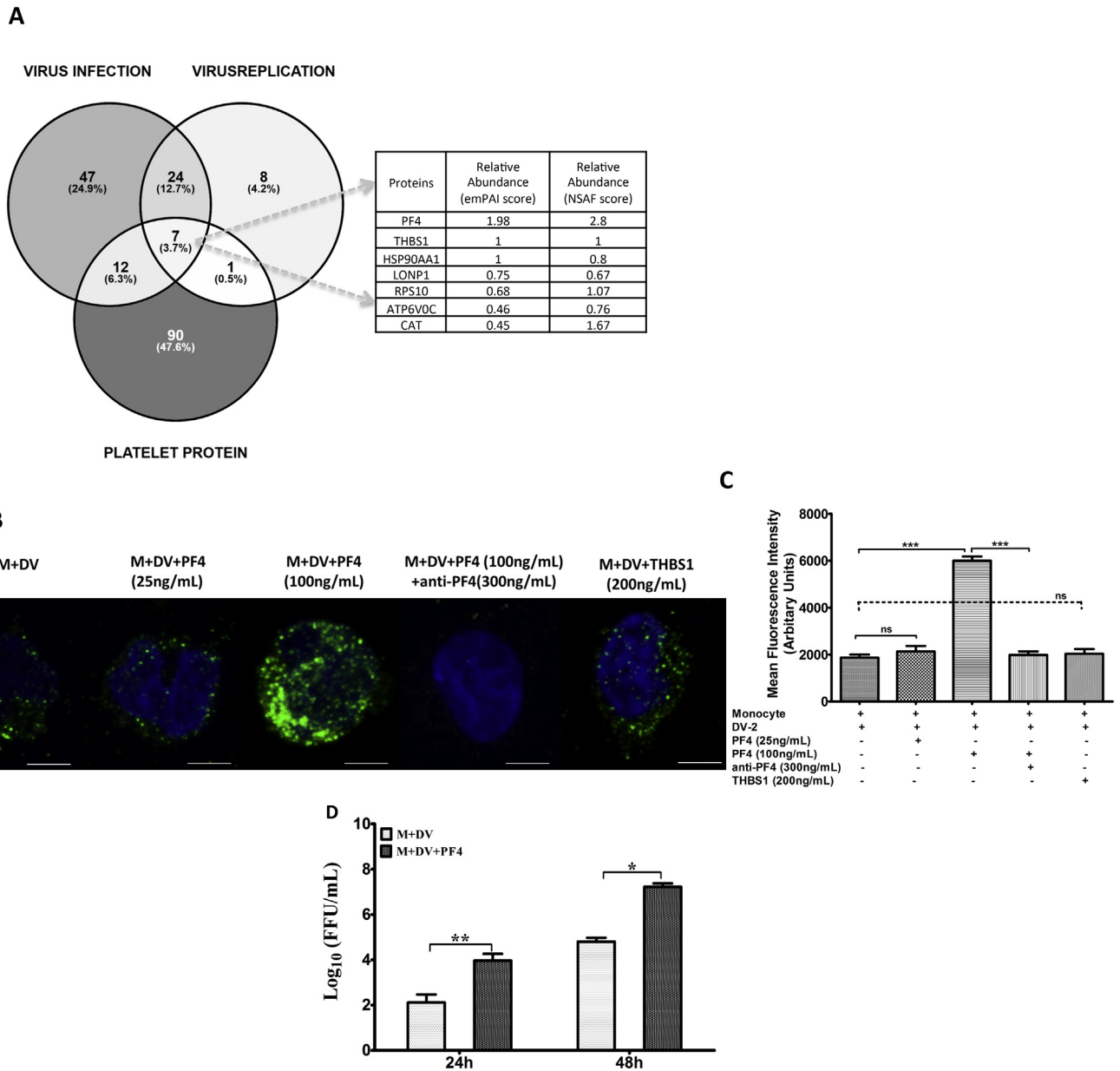


Fig. 2. Platelet factor 4 (PF4) is associated closely with DV2 replication in monocytes. (A) Mass spectrometry analysis of THP-1 cells lysate from similar experiment mentioned in Fig. 1A was processed for density gradient centrifugation to collect the post-nuclear endosome-rich fractions and processed for mass spectrometry analysis using LC-MS/MS. The Venn diagram analysis showed that seven platelet proteins including PF4 (with highest abundance) were associated with proteins from viral replication as well as infection network. The proteins in Venn diagram are mentioned detail in Supplementary Table S3. (B) RhPF4 increased DV2 replication in monocytes *in vitro*. DV2-infected monocytes were incubated for 24 h with various concentrations of rhPF4 (with or without anti-PF4 antibody) or hTHBS1 (thrombospondin-1) instead of platelet or platelet supernatant. The dsRNA was stained (green). (C) MFI of dsRNA from Fig. 2B is presented as mean \pm SEM. One-Way ANOVA was used, $***p < 0.0001$. (D) Infection assay. The supernatant from monocytes incubated with either only-DV2 or DV2 + PF4 was used to infect Vero cells. The FFU was calculated using paired *t*-test as mentioned in Fig. 1G, $*p = 0.0154$, $**p = 0.0033$. (E) Anti-PF4 antibody abrogated DV2 replication in monocytes or THP-1 cells (Fig. S4A and S4B) incubated with DV-activated platelet supernatant. The supernatant of DV-activated platelets was preincubated with anti-PF4 antibody before adding to monocytes and incubated for 24 h. Cells were stained for dsRNA (green). (F) MFI of dsRNA was measured from Fig. 2E and analyzed using One-Way ANOVA, $***p < 0.0001$. (G) AMG487, antagonist of CXCR3 (receptor for PF4) abrogated DV2 replication. The DV2-infected monocytes were incubated with AMG487 (2.5 μ M) for 10 min before adding PF4. The monocytes were incubated for 24 h and dsRNA was measured using microscopy. (H) MFI of dsRNA was measured from Fig. 2G and analyzed using paired *t*-test, $***p < 0.0001$. The AMG487 showed maximum effects at the concentration 2.5 μ M (Fig. S5A and S5B).

pathways, mentioned in Supplementary Table S3. The platelet proteins such as PF4 and thrombospondin (THBS1) were used for further experiments for validating their role in DV replication.

2.19. Flow cytometry

The isolated PBMCs from dengue patients or normal individuals were stained anti-CD14 and then processed for intracellular staining. The cells were fixed with BD Cytofix/Cytoperm fixation and permeabilization kit, and labeled with anti-human CD41 (HIP8) and anti-DV

NS1. The cells were acquired using a FACS Verse (BD Biosciences, San Jose, USA) and data were analyzed using FlowJo software (Treestar, Ashland, USA).

2.20. Cytokine quantification by flow cytometry bead array (CBA)

Cytokine quantification was performed in secretome of treated monocytes as mentioned above. The cytokines such as IFN- α , TNF- α , IL-1 β and IL-6 were measured using CBA assay (BD Biosciences, USA).

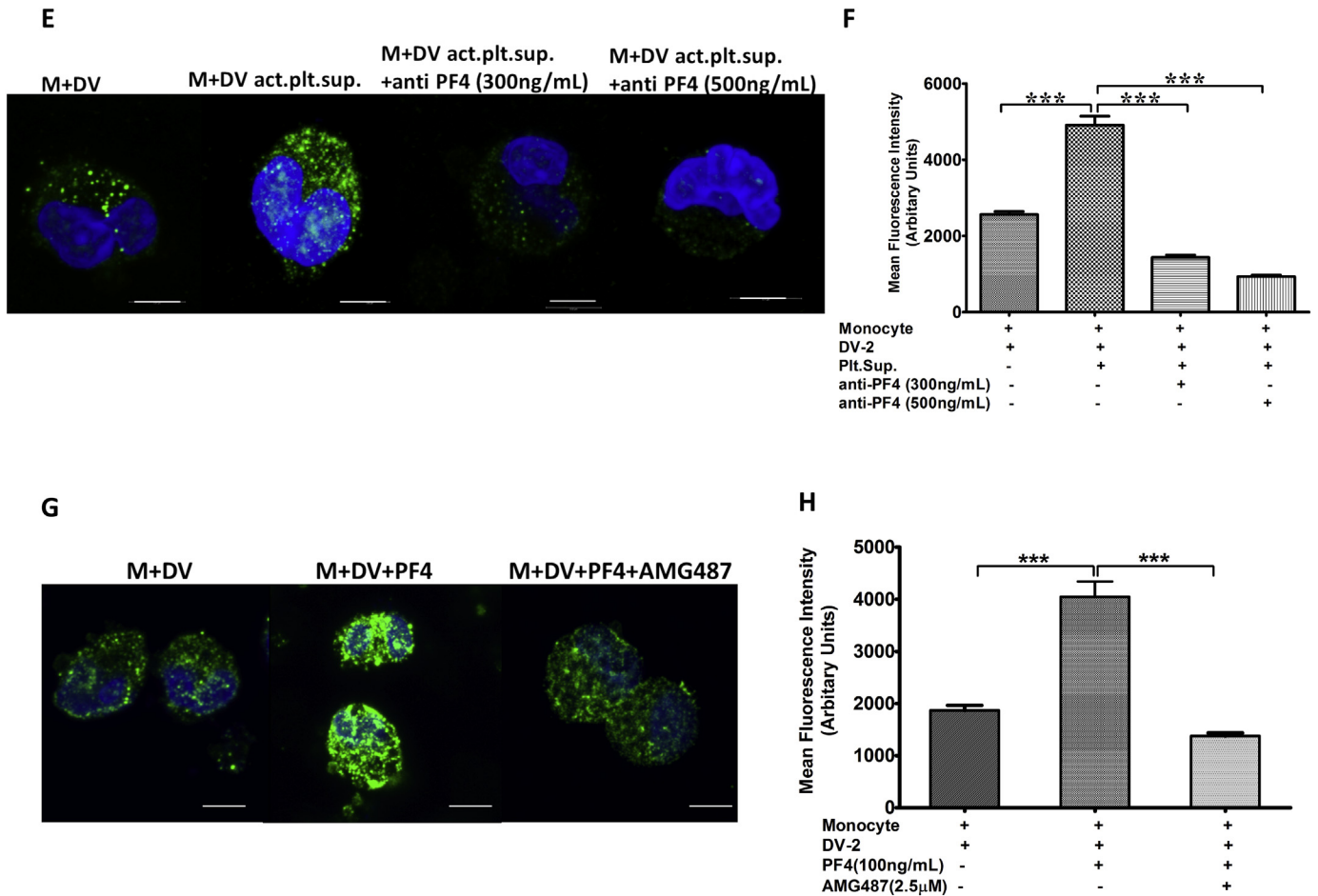


Fig. 2 (continued).

2.21. PF4 quantification by ELISA

The PF4 was measured from plasma of DV patients and normal individuals as well as JEV-infected and normal mice using respective ELISA Kits (R&D Systems, Minneapolis, USA) as per manufacturer's protocol.

2.22. NS1 ELISA

The presence of NS1 in plasma was detected in DV patients using the commercially available qualitative Dengue Early NS1 ELISA kit (PanBio, Brisbane, Australia) as per manufacturer's protocol.

2.23. Immunoblotting

The intracellular signaling proteins were detected in monocytes from above treatments for 24 h as mentioned in section 2.7. The cell pellets were lysed with RIPA buffer supplemented with Halt™ protease-phosphatase inhibitor (Thermo Scientific Life Technologies, Omaha, USA). The lysis products were processed for SDS PAGE and immunoblotting for the signaling molecules such as phospho and non-phospho p38, STAT-2 and NFκB, and IκBα, IRF-9 and β-actin.

2.24. Statistical analysis

The experimental values from at least three independent experiments were presented as mean ± standard error (SEM) for all results unless mentioned. Statistical analysis was performed using either paired *t*-test or one-way ANOVA. For dengue patient's sample

experiments Mann Whitney *U* test was used for comparison between different day points. An unpaired *t*-test was used for comparison between control and test mice groups. One-way ANOVA followed by Bonferroni's *post hoc* test was used for mice survival study. Graph Pad Prism 5.0 software was used for data analysis and *P* values < 0.05 were considered to be statistically significant.

3. Results

3.1. Enhanced replication and propagation of DV2 in monocytes in presence of platelets or platelet supernatant in vitro

Since virus replication uses host cellular machinery, we have investigated the differences in Dengue virus type-2 (DV2) replication in monocytes when these immune cells 1) engulfed either only DV2 or 2) DV2-activated platelets, or 3) incubated with supernatant of DV2-activated platelets (detail experimental design in section 2.7). We observed that the level of dsRNA (detail quantification method in section 2.9) corresponding to DV2 replication intermediate was 4-fold higher at 24 and 48 h in monocytes that engulfed DV2-activated platelets than the counterparts engulfed only DV2 (Fig. 1A and B). High level of dsRNA colocalized with platelets in monocytes (Fig. 1C and D). Our PCR data also showed the equal copies of DV2 genome at 2 h in monocytes pellet either collected from treatment with only-DV2 or DV2-activated platelets, but the DV2 genome copy increased significantly after 24 and 48 h in case of 2nd treatment (Fig. 1E). A similar result was observed when the above experiments were performed using a monocytic cell line, THP-1 (Fig. S1A and S1B). Further, our data showed that the

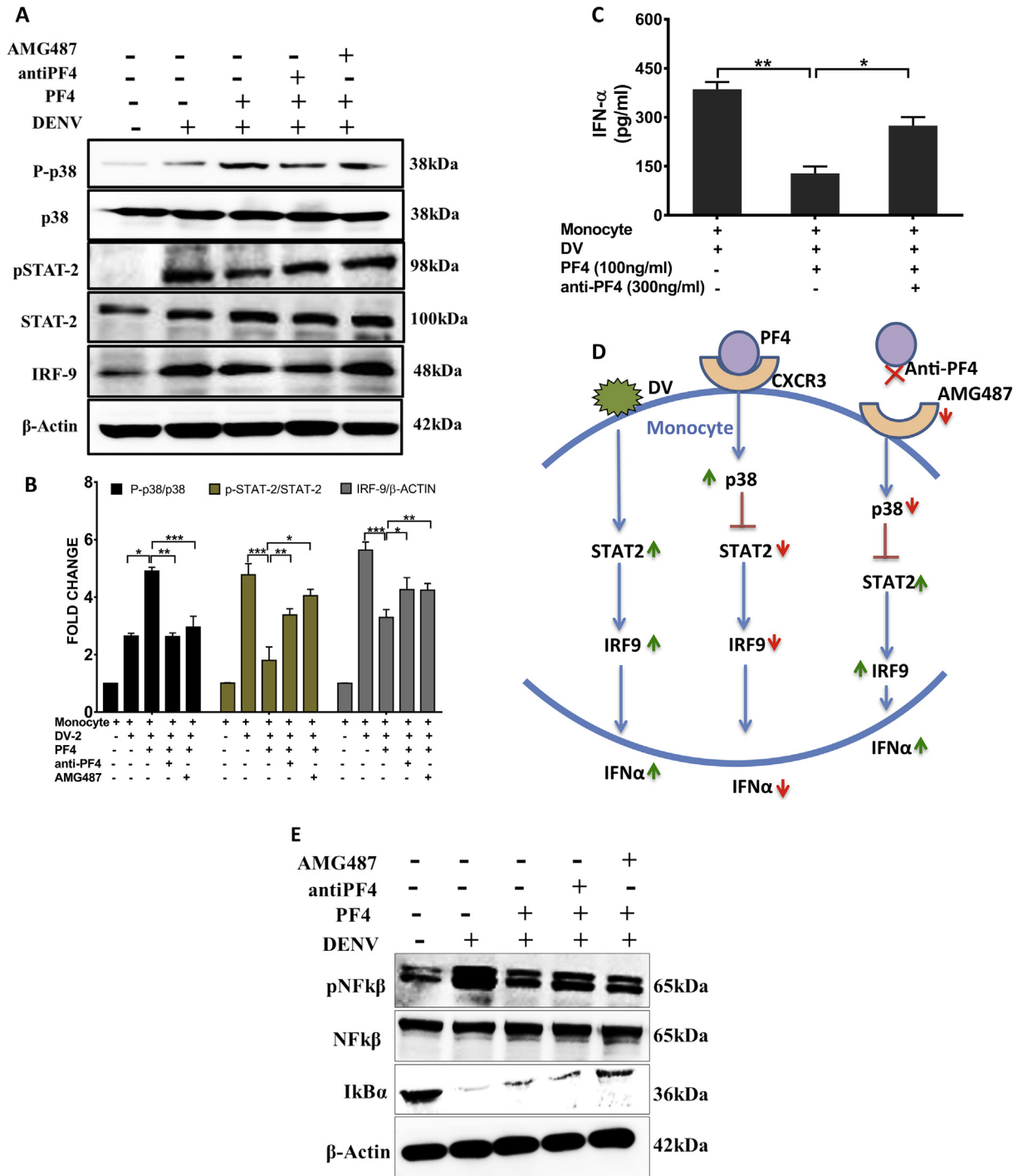


Fig. 3. PF4 inhibits STAT-2 – IRF-9 pathways and decreases interferon secretion from monocytes. (A) The monocyte pellets were collected from experiments where cells were incubated with DV2 + PF4 with or without anti-PF4 or AMG487. Cell lysate was used for quantifying phospho and non-phospho p38 and STAT-2, and IRF-9 and β-actin using immunoblotting. (B) The densitometry data from above such three experiments are presented as mean ± SEM and analyzed using paired t-test, for p38: **p* = 0.0074, ***p* = 0.003, ****p* = 0.0037; for STAT2: **p* = 0.0291, ***p* = 0.027, ****p* = 0.013; for IRF: **p* = 0.0313, ***p* = 0.0024, ****p* = 0.0001. (C) The IFN-α was measured from supernatant of above experiments using the flow cytometry based array (CBA). Data are mean ± SEM from five different experiments. Paired *t*-test was used, **p* = 0.02, ***p* = 0.0091. (D) Schematic represents the PF4-mediated IRF-IFN pathway. (E) The phospho and non-phospho NFκB, and IκBα was also measured from the cells pellet from Fig. 3A. (F.a) Densitometry data of Fig. 3E, **p* = 0.01, ***p* = 0.0093 (anti-PF4), ***p* = 0.0013 (AMG487) (F.b) **p* = 0.0196, ***p* = 0.0019. (G) Inflammatory cytokines such as TNF-α, IL-1β and IL-6 were measured from cell supernatant from above experiment using CBA and data were analyzed, **p* = 0.0008 and **p* = 0.0007 compared to respective parameters from monocytes treated with DV; ***p* = 0.0002 and ****p* < 0.0001 compared to respective parameters from monocytes treated with DV + PF4.

monocytes (1×10^5 /well) when engulfed more number of platelets (1×10^7 /well) mixed with 3×10^7 PFU DV2, displayed elevated expression of intracellular NS1 compared to monocytes that engulfed less platelets (0.25×10^7 /well) with same MOI (3×10^7 PFU) of DV2 (Fig.1F and 1G). These results together suggested the significant contribution of platelets in enabling DV2

replication in host immune cells. Besides, we observed that monocytes, which engulfed DV2-activated platelets produced elevated amount of new virion particles and infected Vero cells potentially compared to the titre from only DV2-infected monocytes (Fig.1H), indicating the direct role of platelet proteins in enhanced DV2 propagation.

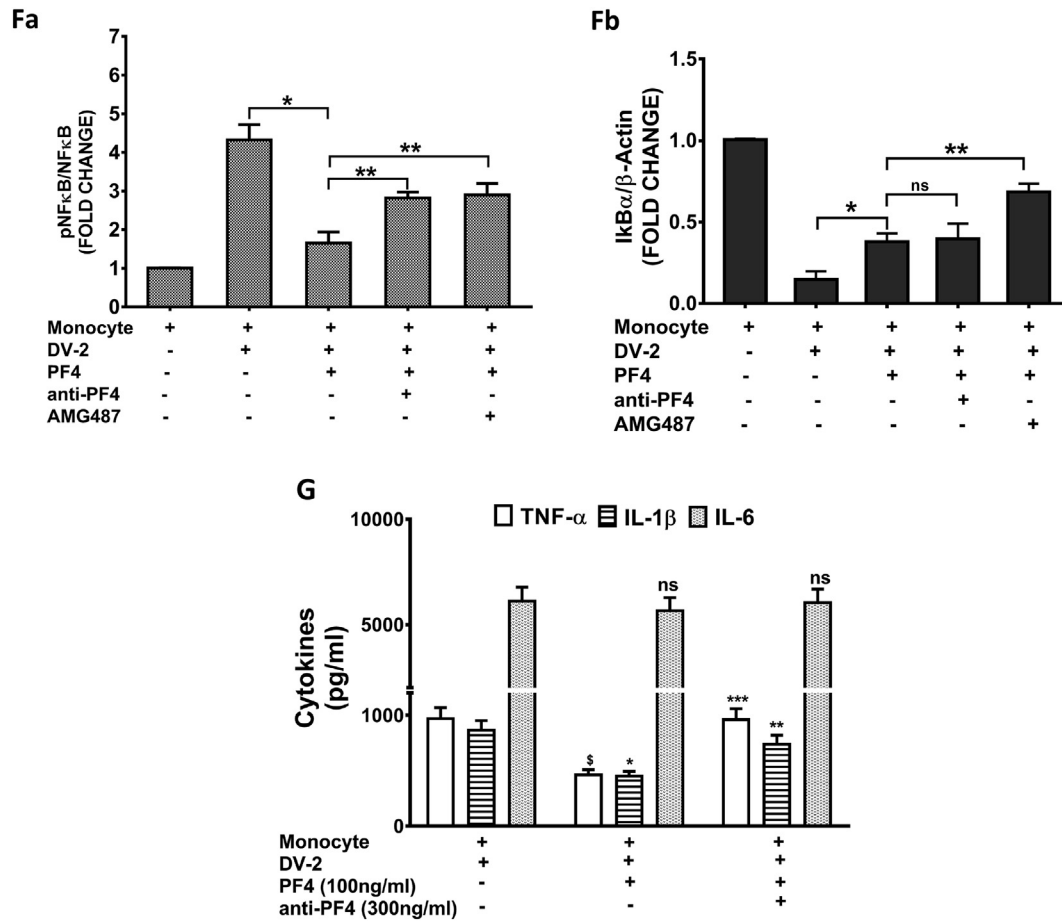


Fig. 3 (continued).

3.2. Platelet protein PF4 showed close association with the DV2 replication and propagation

To identify the platelet protein(s) involved in DV2 replication we have performed proteomic analysis of post-nuclear fractions of THP-1 cells from above treatments (mentioned in Fig. S1). The proteomic study using mass spectrometry followed by gene ontology biological processes-based enrichment analysis revealed that the platelet factor 4 (PF4) was highly abundant in THP-1 cells that exhibited elevation in viral replication after engulfing DV2-activated platelets (Fig. 2A). Further, we investigated the role of purified PF4 or thrombospondin-1 (THBS1) in DV2 replication. Our data showed that in presence of recombinant human PF4 (rhPF4) the DV2-infected monocytes (1×10^5 cells/well infected with 3×10^7 PFU DV2) displayed enhanced dsRNA staining in a concentration-dependent manner with a maximum 3-fold increase at 100 ng/mL, a relevant concentration reported in Dengue patients' plasma [11] (Fig. 2B and C). A similar observation was made in THP-1 cells that showed maximum stimulatory effects of rhPF4 (at 100 ng/mL) on DV2 replication (Fig. S3A and S3B). More importantly, the presence of other platelet protein such as thrombospondin-1 (THBS1) did not increase the DV2 replication in monocytes (Fig. 2B and C). Likewise, another platelet protein fibrinogen (FGA) also did not show any alteration in DV2 replication in monocytes (data not shown). Further, our data showed that newly synthesized virion particles from DV2-infected monocytes incubated with rhPF4, were capable of infecting Vero cells potently (Fig. 2D) suggesting the role of platelet protein PF4 as the major enhancer of DV2 propagation and infection in host.

3.3. Antibody to PF4 or antagonists to PF4 receptor CXCR3 abrogated DV2 replication in monocytes in vitro

Further, our data showed that the anti-PF4 antibody inhibited the PF4-induced elevation of DV2 replication in monocytes (Fig. 2B and C). Data also showed that the anti-PF4 antibody at 300 ng/mL concentration inhibited significantly the DV2 replication in monocytes or THP-1 cells incubated with the supernatant of DV2-activated platelets. The higher concentration of antibody (500 ng/mL) abrogated the viral replication in monocytes (Fig. 2E and F and Fig. S4 A and S4 B). Our study also examined the effect of an antagonist to CXCR3 (receptor for PF4), namely AMG487. AMG487 at 2.5 μ M (1.5 μ g/mL) significantly inhibited the PF4-induced DV2 replication in monocytes (Fig. 2G and H). Similar observation in monocytic THP-1 cells also confirmed PF4 as the major platelet protein, which promoted DV2 replication (Fig. S5A and S5B). Although, AMG487 significantly inhibited PF4-mediated elevation in DV2 replication in monocytes/THP1 cells, but did not effect the DV2 replication in these cells in absence of stimulus such as PF4 or activated-platelets (Fig. S6A and S6B). Our data also showed that AMG487 treatment (1 or 2.5 μ M) did not alter the cell survival (Fig. S7).

3.4. PF4 inhibited the DV2-induced interferon (IFN) secretion from monocytes in vitro

To investigate further the mechanism our data showed that rhPF4 significantly inhibited the anti-viral response of the DV2-infected monocytes. The PF4 increased the phosphorylation of p38MAPK and in turn inhibited the activation of STAT-2 and IRF-9 (Fig. 3A and B)

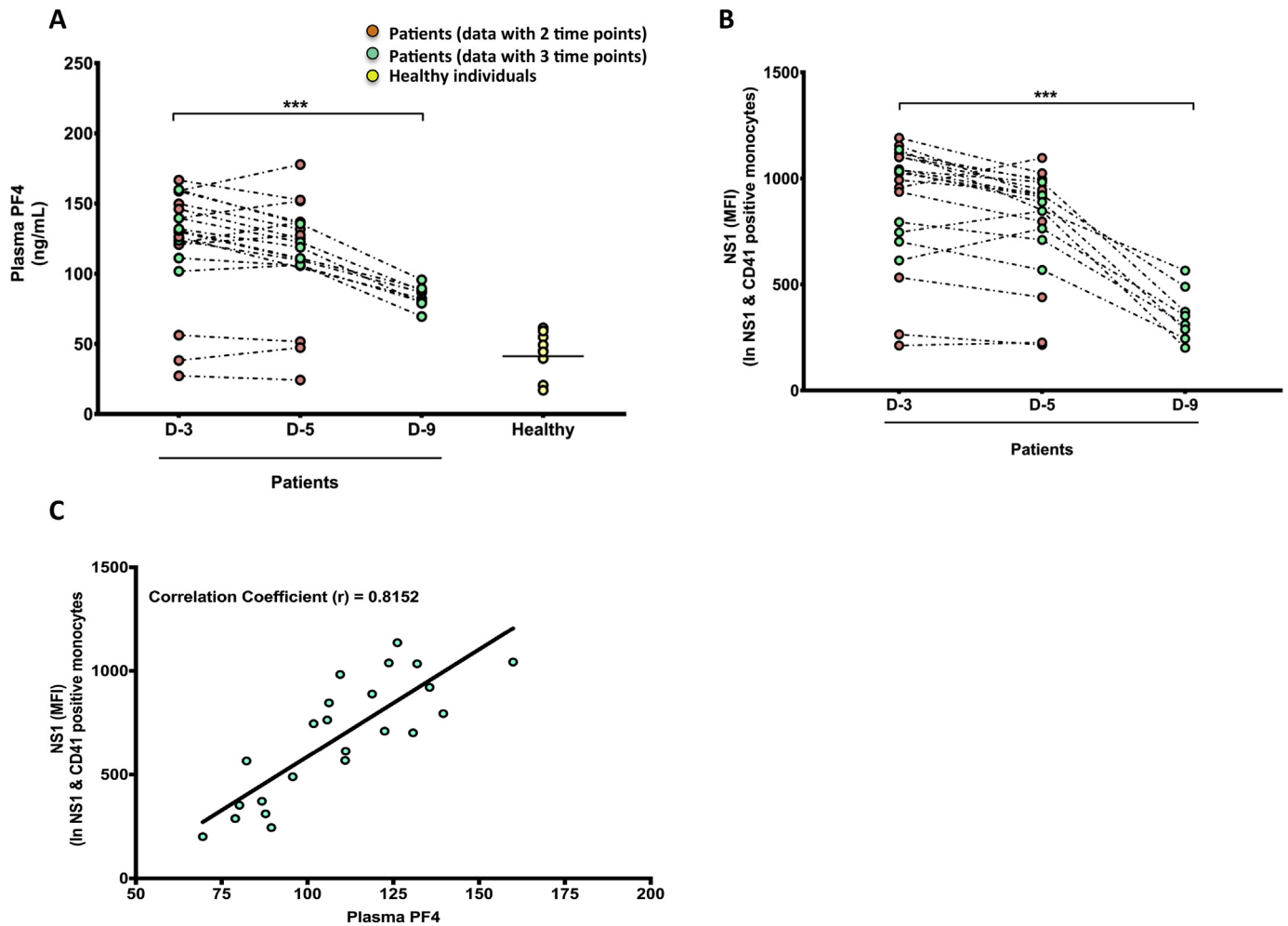


Fig. 4. Elevated PF4 in plasma coexists with high NS1 in monocytes in DV patients. (A) Plasma was collected from DV patients ($n = 20$) at day-3 (or Day-1 of hospitalization) and day-5 of fever. Only 8 of the 20 patients were followed till day-9. Plasma PF4 level was measured using ELISA kit. Healthy individuals' ($n = 10$) plasma was used as the normal reference. Each dot represents each patient's data; green dots represent 8 among 20 patients. Mann Whitney U test was used, $***p = 0.0002$ between day-3 and day-9 data of 8 patients. (B) PBMCs were collected from above patients on mentioned days. Using flow cytometry the intracellular NS1 (MFI) was measured in the $CD41^+NS1^+$ monocytes. Mann Whitney U test was used, $***p = 0.0002$ between day-3 and day-9 data of 8 patients for both Fig. 4B and C. The flow cytometry plot is mentioned in Fig. S9. (C) Correlation coefficient between plasma PF4 and NS1 (MFI) in monocytes of 8 patients from day-3/5/9. (D) Monocytes from 3 of the above 8 patients (P 1–3) at day-3 (D3) and day-9 (D9) were stained for intracellular viral dsRNA (green) nucleus (blue) using microscopy. The monocytes of 2 healthy individuals (H1–2) were used for staining. (E) Quantification (MFI) of dsRNA from 10 images from each day point of each patient, mentioned in Fig. 4D. Data presented as mean \pm SEM. Unpaired t -test was used for analysis, $*p = 0.0003$, $***p = 0.0001$.

and finally decreased the synthesis and secretion of IFN- α in the DV2-infected monocytes (Fig. 3C). More importantly, the presence of either anti-PF4 antibody or antagonist to PF4 receptor CXCR3, AMG487 reversed the above pathway and restored the IFN- α secretion in DV2-infected monocytes (Fig. 3A and D). Also our data showed that rhPF4 inhibited the inflammatory response of these DV2-infected monocytes. RhPF4 significantly decreased phosphorylation of NF- κ B and parallel increased I κ B- α expression (Fig. 3E and Fa-b), and affected the secretion of cytokines such as TNF α , IL-1 β and IL-6 in monocytes (Fig. 3G). As expected, the anti-PF4 antibody treatment reversed the above pathway and restored the secretion of above cytokines in DV2-infected monocytes (Fig. 3G).

3.5. High plasma PF4 coexisted with high levels of intracellular NS1 in monocytes from Dengue patients during day-3/5 of fever

Further our data from Dengue patients ($n = 20$, patients' detail is mentioned in Supplementary Table S1) showed that higher plasma levels of PF4 [average 122 ng/mL ($n = 20$) during day-3 and 115 ng/mL ($n = 20$) during day-5 (reference for plasma PF4 in normal

healthy individuals ($n = 10$) with an average 41 ng/mL, Fig. 4A)] coexisted with high level of intracellular DV NS1 protein in monocytes (Fig. 4B) during day-3 and day-5 of fever [these patients were admitted to hospital during day-3 of fever with NS1 positivity in plasma and low platelet counts (Supplementary Table S1)]. Further, our data showed significantly decreased levels of plasma PF4 in 8 out of 20 patients (as mentioned above) at day-9 with an average 84 ng/mL compared to day-3 (average 128 ng/mL) and day-5 (average 116 ng/mL; Fig. 4A). The plasma PF4 level (Fig. 4A) showed the direct correlation (correlation coefficient, $r = 0.8152$) with the levels of intracellular NS1 in monocytes (Fig. 4C) and an inverse correlation ($r = -0.664$) with platelet counts (Fig. S8) in above 8 patients. Although, our data showed the complete absence of NS1 protein in plasma of these 8 Dengue patients at day-9 (Supplementary Table S1). Furthermore, our microscopy data depicted the elevated staining of intracellular dsRNA in peripheral monocytes from patients at day-3 of fever compared to the counterparts from same patients at day-9 (Fig. 4D and E). The monocytes from healthy individuals ($n = 10$) did not display intracellular staining for NS1 analyzed using flow cytometry (data not shown). These healthy individuals ($n = 5$) did not show staining for intracellular staining for

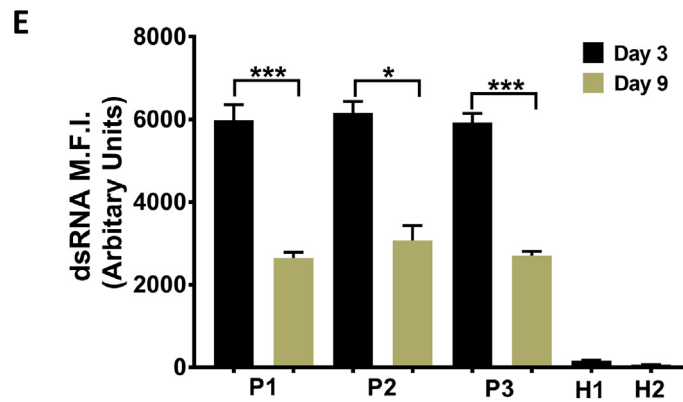
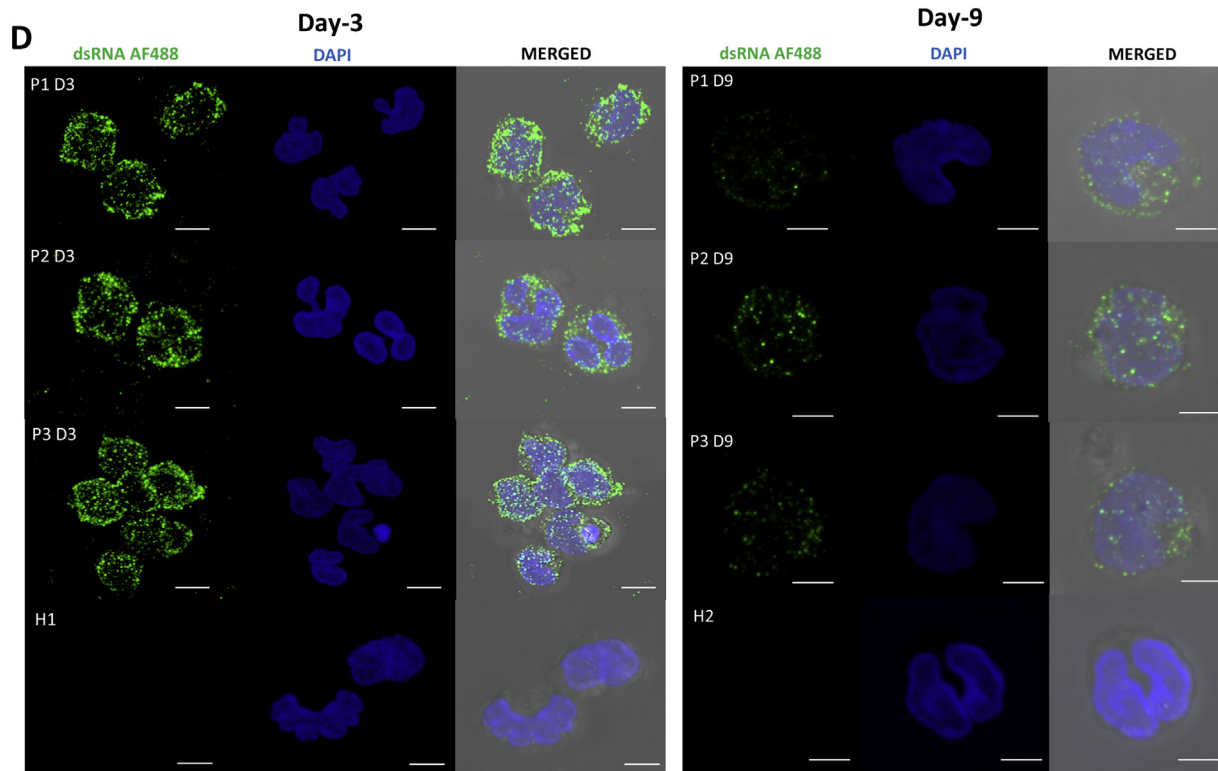


Fig. 4 (continued).

dsRNA assessed using microscopy (data for 2 out of 5 is mentioned in Fig. 4D and E). The above observations together indicated clearly a direct association between plasma PF4 and viral replication in monocytes in Dengue patients.

3.6. PF4 also promoted JEV replication in human monocytes and mouse microglia cells *in vitro*

In order to investigate whether PF4-mediated mechanism of viral replication exists in other flaviviruses, we observed that the replication of a related virus, JEV increased about 2-fold in human monocytes (Fig. 5A and B) after 24 h of JEV infection (GP78 strain, 3×10^7 PFU) in presence of rhPF4 (100 ng/mL). As expected the treatment of either anti-PF4 antibody (300 ng/mL) or AMG487 (2.5 μ M) significantly reduced the viral replication, as well as, increased the IFN- α secretion in JEV-infected monocytes (Fig. 5A, B and C). Similarly, in presence of rhPF4 the JEV replication was significantly increased in mouse microglia BV2 cells (Fig. 5D and E). Effectivity of hPF4 in mouse BV2 cells might be because of high sequence homology (65%) between hPF4 and mouse variant, mPF4. Our data also showed that the treatment of CXCR3

antagonist AMG487 (2.5 μ M) significantly inhibited the PF4-mediated JEV replication in BV2 cells (Fig. 5D and E).

3.7. AMG487 treatment in mice reduced JEV infection and increased mice survival

Our study further examined the *in vivo* effects of AMG487 in mice infected with JEV. Injection (i.p) of AMG487 (4 mg/kg body twice daily) starting from 12 h before JEV infection with 3×10^5 PFU till day-3 (expt.-1) or day-5 (expt.-2; Fig. 6A graphical study design) to mice, significantly rescued the infection. The AMG487 treatment for 3 or 5 days significantly decreased the levels of JEV NS3 protein in brain tissues (Fig. 6B1 and 6B2, and 6C). Further, the plaque assay showed that the lysate from brain tissues of JEV-infected mice with AMG487 treatment, was about 10-fold less infectious than the brain lysate of JEV-infected mice (Fig. 6D) indicating clearly the reduction of viral load following this drug treatment. Our data also showed that the plasma PF4 level in BALB/c mice increased significantly after day-3 of JEV infection (from 1500 ng/mL to 2991 ng/mL) and remained unaltered after the AMG487 treatment (Fig. 6E). Interestingly, the expression of IFN α

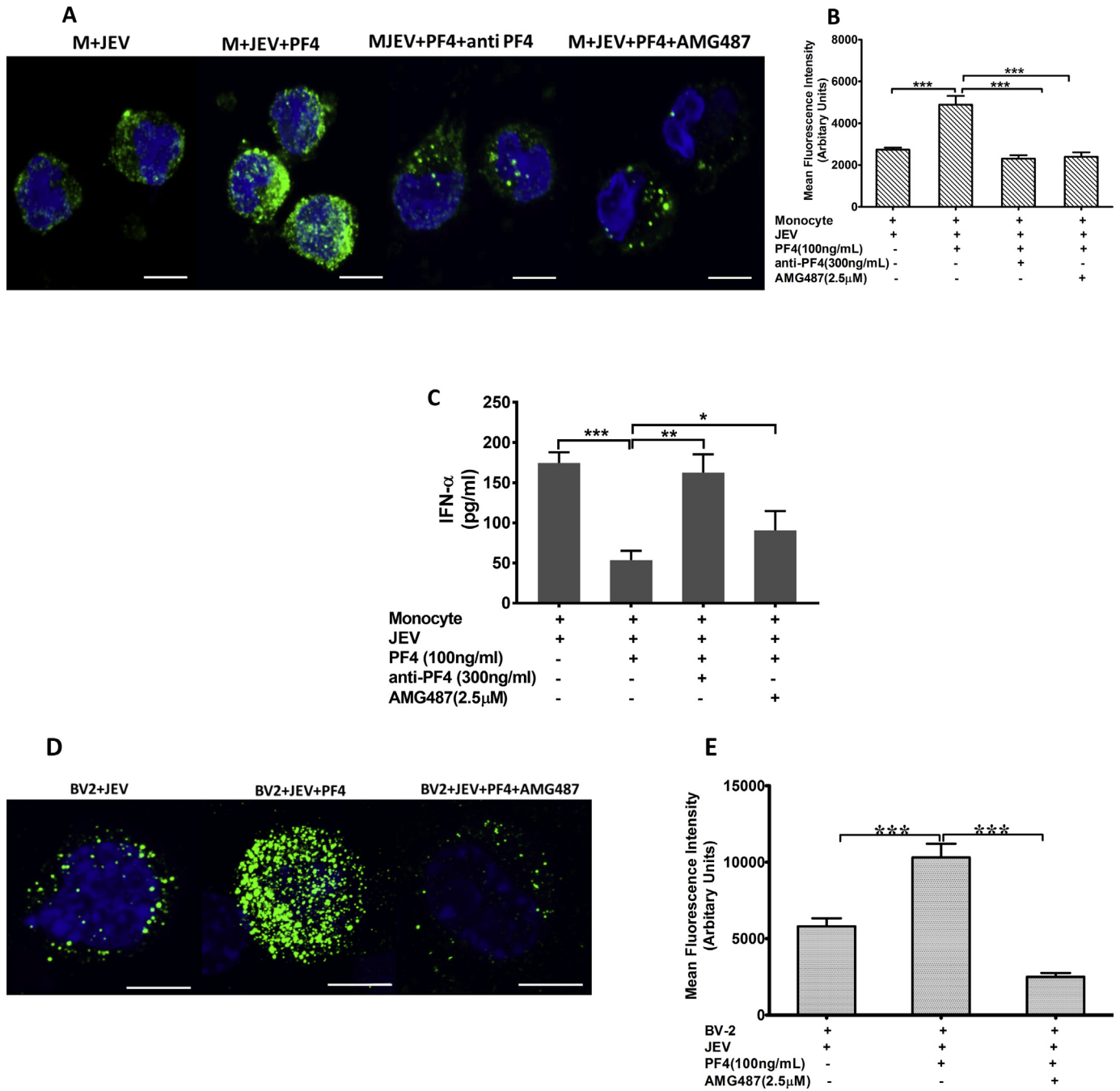
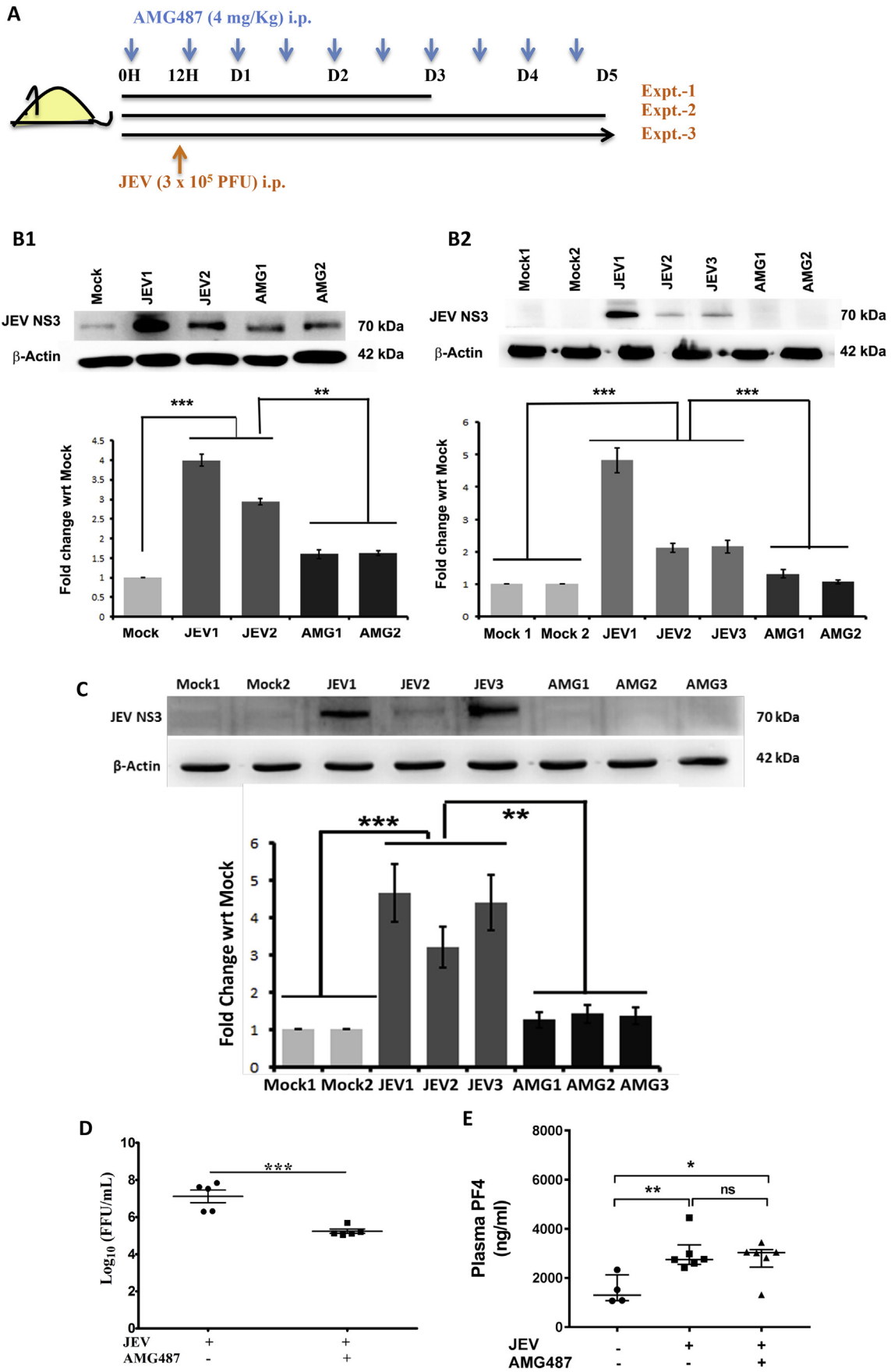


Fig. 5. PF4 increases JEV replication in human monocytes and mouse microglia cells *in vitro*. (A) Freshly isolated monocytes from healthy individuals were incubated with JEV (strain GP78, 24 h) in presence of rhPF4 with and without anti-PF4 antibody or AMG487. Cells were stained for dsRNA (green). (B) The MFI of dsRNA was measured using paired t-test, $***p < .0001$. (C) The IFN- α was measured from supernatant of monocytes from above experiment using CBA. Data are represented as mean \pm SEM from three different experiments. Paired t-test was used, $*p = .0136$, $**p = .0011$, $***p \leq .0001$. (D) Similarly, the mouse microglia BV2 cells were incubated with JEV for 24 h in presence of rhPF4 with or without AMG487 and stained for dsRNA. (E) The MFI of dsRNA was measured using paired t-test as mentioned in Fig. 2D, $***p < .0001$.

(Fig. 6F1 and 6F2) as well as interferon-stimulated gene-15 or *ISG-15* (Fig. S10A and S10B) was decreased in brain tissues of JEV-infected mice, but rescued following AMG487 treatment. Besides, the JEV-infected mice displayed reduced body weight and developed encephalitic symptoms on day-5 onwards. All JEV-infected mice died between day-6 and 7, but the AMG487-treated mice displayed delayed development of encephalitic symptoms and increased survival. >50% mice survived till day-9 post infection and >30% survived till day-11. Interestingly, 20% of the AMG487-treated mice started developing encephalitis like symptoms post day-5 of JEV injection, but they

gradually recovered and survived (Fig. 6G). The survived mice were carefully monitored till day-20 post infection for any behavioral alterations. These mice were sacrificed on day-20 and viral titre was estimated in brain tissues. The brain tissue lysate of these mice displayed 40-fold reduced efficiency in infecting the Vero cells (Fig. 6H) due to high recovery and persistence of low viral load following AMG487 treatment. We also confirmed low viral titre in these animals by estimating 6–7 fold less number of JEV genome copies in organs such as liver, spleen and blood cells compared to the JEV-infected group (Fig. 6I).



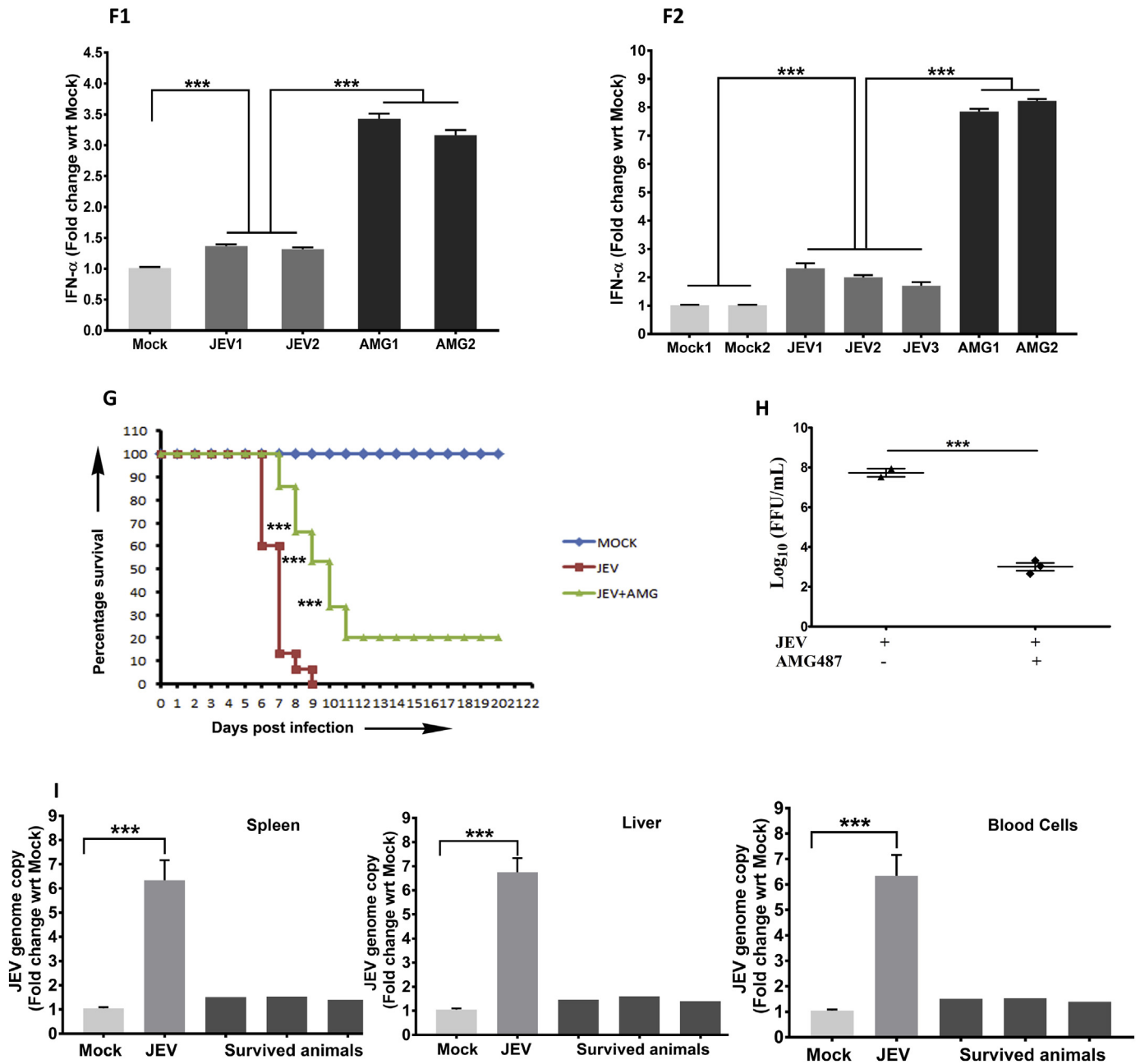


Fig. 6. AMG487 inhibits JEV infection and increases mice survival. (A) Mice were injected with AMG487 twice daily starting 12 h before the JEV injection. In three different experiments, mice were injected with AMG487: 1) till day 3 and sacrificed at day 4; 2) till day 5 and sacrificed at day 6; and 3) till day 5 and allowed for survival. (B.1–2). Brain tissue from mice ($n = 12$) from above experiment-1 (from two separate experiments) was used for measuring the viral protein NS3 using immunoblotting. Bar represents the densitometry data of the blots in relative fold change in NS3 expression compared to mock animals. Statistical analysis was performed using One-Way ANOVA, $**p < 0.01$, $***p < 0.001$. (C) NS3 immunoblot data of brain tissue of mice ($n = 8$) from experiment-2. Bar represents the densitometry data of the blots in relative fold change in NS3 expression, $**p < 0.01$. (D) Infection assay- lysate of brain tissue from mice from experiment-1 was used to infect Vero cells and FFU was measured. Data were analyzed using unpaired t-test, $***p = 0.0007$. (E) Plasma PF4 level was measured from plasma of mice from experiment-1, using ELISA kit. Each dot represents each mouse data. Data were analyzed using Mann Whitney U test, $*p = 0.038$, $**p = 0.0095$. (F) The IFN α gene expression was measured using qPCR from mice brain tissue from experiment-1. Data present fold-change compared to mock. Data analyzed using One-Way ANOVA, $***p < 0.0001$. Similar data of ISG-15 gene expression are mentioned in Fig. S10. (G) Mice survivability. As mentioned above the experiment-3 was performed to assess the survival rate and p -value was determined by One-Way ANOVA followed by Bonferroni's *post hoc* test; $***p < 0.001$ between groups during various days. The AMG487 treatment increased significantly survival of JEV-infected mice ($n = 15$) beyond day-6. 20% mice survived. (H) Infection assay was performed using lysate of brain tissue from 20% mice that survived from above experiment as in Fig. 6F. These mice were sacrificed at day-20 and brain tissue lysate was used to infect Vero cells. Data were analyzed as mentioned in Fig. 6D, $***p < 0.0001$. (I) The JEV genome copy was measured using qPCR from the organs such as spleen, liver and blood cells of 20% survived mice as mentioned in Fig.6F. Data were analyzed using One-Way ANOVA, spleen $***p = 0.0001$, liver $***p = 0.0004$, blood cell pellet $***p = 0.0002$.

4. Discussion

Our study delineates the unique role of platelet cytokine PF4 in enhancing the replication as well as propagation of closely related flaviviruses such as DV and JEV in host cells. Our *in vitro* data showed that upon incubation with DV-activated platelets, monocytes (isolated

from healthy individuals) or monocytic THP-1 cells displayed 3–4-fold increase in DV2 replication at 48 h compared to counterparts infected with only DV2, although the DV2 genome copies were similar at 2 h in monocytes pellet from both treatments. Importantly, monocytes (1×10^5 /well) incubated with more number of platelets (1×10^7 /well) along with 3×10^7 PFU DV2, displayed significantly elevated viral

replication than the monocytes incubated with less platelets (0.25×10^7 /well) but same MOI of virus, indicating clearly the contribution of platelet protein(s) in DV2 replication. With the help of proteomic analysis, we have identified the association of a host protein platelet factor-4 (PF4) with the enhanced replication of DV2 in THP-1 cells. The presence of recombinant hPF4 at 100 ng/mL, a relevant concentration in plasma of Dengue patients [11] in supernatant, induced the similar fold increase in DV2 replication in monocytes *in vitro* as observed for monocyte counterparts treated with supernatant from DV2-activated platelets. Further, the presence of anti-PF4 antibody in the supernatant of DV2-activated platelets significantly abrogated the viral replication in monocytes *in vitro* and confirmed PF4 as the major cytokine secreted from activated-platelet enabling significantly enhanced replication of DV2 in host cells.

Our above study thus described PF4, secreted specifically from activated platelets, as the potent enhancer of DV replication in host cells including monocytes. PF4 is released from the α -granules of activated platelets and contributes to the progression of thrombosis or clot formation by neutralizing the anti-coagulant effects of heparin on vascular endothelium [41]. Besides, PF4 also plays important role as the chemoattractant in the progression of processes such as tissue inflammation and cellular homing [42,43]. Studies also have described the role of PF4 as the inhibitor or enhancer for HIV-1 [12,44], and modulator for H1N1 [15] infections in human. Our study described for the first time a direct association of PF4 in enhancing rapidly the DV replication in monocytes. The virion particles produced from DV2-infected monocytes in presence of PF4, displayed potent infectivity towards other cells. Our above study thus suggested the crucial role of PF4 in enabling the elevated propagation of DV2 in host immune cells *in vitro* within a short window of 24–48 h.

Virus replicates as well as propagates in cytosol of host cells and host immune response induces the interferon (IFN) secretion, which further inhibits the entry of virus to other cells [28,29]. Our data described that the addition of rhPF4 in the culture of DV2-infected monocytes significantly inhibited the secretion of IFN- α in monocytes via p38 MAPK - STAT-2 - IRF-9 pathways and enhanced DV2 replication in these cells. Besides, rhPF4 also inhibited the synthesis and secretion of other inflammatory cytokines such as IL-1 β , IL-6 and TNF- α in monocytes via I κ B- α -NF κ B axis. As expected the above secretion machineries in monocytes were rescued when the cells were pretreated either with anti-PF4 antibody or the antagonist to PF4-receptor, CXCR3 or CXCR3B (a spliced variant of CXCR3). Thus our data suggested the role of PF4 in enabling the DV2 replication and propagation in monocytes by limiting the host's anti-viral interferon response. Further our data from Dengue patients described the direct correlation between elevated plasma PF4 (122 ng/mL) and high intracellular DV2 NS1 protein in peripheral monocytes at day-3 compared to day-9 of infection, and supported the association of PF4 with rapid propagation of DV2 in host *in vivo*. Besides, our data also exhibited the inverse correlation between high plasma PF4 and low platelet counts in these patients, indicating further the formation of elevated immunogenic PF4-heparin complexes and in turn induction of thrombocytopenia during initial days (between 2 and 5 days) of Dengue infection [45].

In order to investigate whether the above mechanism exists in other viruses, we observed that PF4 enhanced significantly the replication of another closely related flavivirus JEV in monocytes by limiting IFN- α synthesis in these cells *in vitro*. As expected, the pre-treatment with either anti-PF4 antibody or AMG487 rescued the IFN- α secretion and significantly inhibited the JEV replication in monocytes. In a similar observation, PF4 significantly increased the JEV replication in mouse microglia cells, which was further decreased by AMG487 *in vitro*. In order to investigate the role of PF4-CXCR3-IFN axis in viral replication *in vivo*, we have tested the CXCR3 antagonist drug, AMG487 in the JEV-infected BALB/c mice, which is a well-established animal model that mimics the robust pathophysiology of the disease [46]. On the other hand, such animal model for DV infections is an obstacle, more importantly for investigating the involvement of PF4-CXCR3-IFN axis

in DV infection *in vivo*, is a challenge because of non-availability of an immunosufficient small animal model that mimics this viral infection [47]. The CXCR3 antagonist AMG487 is widely used drug, tested in mice models [7,48–50] to inhibit mainly the chemotactic effects of cytokines such as CXCL-9/10/11 (via CXCR3) on cell migration to the site of tumor or atherosclerotic plaque.

We observed that AMG487 injection (twice daily at 4 mg/kg body weight, intraperitoneally) in mice decreased significantly the JEV infections and increased their survival. All JEV treated mice developed encephalitic symptoms at day-5 and died between day-6 and 7. These JEV-infected mice displayed significant elevation in plasma PF4 level inversely with the IFN α or ISG-15 expression in brain tissue. The AMG487 treatment rescued the IFN α as well as ISG-15 expression in brain and reduced infection in these mice. The AMG487 treatment significantly delayed the development of encephalitic symptoms in these infected mice. >50% mice survived till day-9 post infections and >30% survived till day-11. The 20% of the AMG487-treated mice developed encephalitis like symptoms post day-5 of JEV injection, but they gradually recovered and survived. These mice were sacrificed at day-20 and displayed very minimum infection in brain and least copies of JEV genome in spleen, liver and blood cells, suggesting a clear inhibitory effect of AMG487 on JEV propagation and infection in mice.

Therefore, our above observations together suggest the crucial role of platelet cytokine PF4 as the rapid enhancer of replication as well as propagation of both DV and JEV in host cells including monocytes by inhibiting IFN response of these immune cells. We believe that other viruses may utilize the PF4-mediated mechanism for their propagation in host in a situation where PF4 level in circulation is increased due to platelet activation during infections. Definitely the PF4-CXCR3-IFN axis is a potential target for developing treatment regimens against viruses including DV and JEV. Antagonists to CXCR3 including AMG487 can be useful for treatment against JEV and DV, and may be for other viruses.

Author contributions

Amrita Ojha and Prasenjit Guchhait have designed whole study. Amrita Ojha has performed most of the experiments and was involved in other experiments. Angika Bhasym (RCB) has performed all flow cytometry based assays. Sriparna Mukherjee and Anirban Basu (NBRC) have designed the mice experiment. Sriparna Mukherjee and Irshad Akbar have performed mice experiments and related data analysis. Teena Bhakuni, Tulika Seth and Naval K Vikram have recruited dengue patients and collected clinical data and performed related assays. Amrita Ojha has performed mass spectrometry experiment, and Amrita Ojha and Gowtham Kumar Annarapu have analyzed data. Sudhanshu Vrat and Sankar Bhattacharyya have designed virus related experiments and Sankar Bhattacharyya has performed the virus assays and analyzed data. Amrita Ojha and Prasenjit Guchhait have performed final analysis of data. Prasenjit Guchhait was responsible for oversight of the project and preparation of the final manuscript.

Supplementary data to this article can be found online at <https://doi.org/10.1016/j.ebiom.2018.11.049>.

Conflict of interests

Authors do not have any financial or other disclosures.

Sources of funding

This study was financially supported by grants: BT/PR8591 from the Department of Biotechnology, Govt. of India to Prasenjit Guchhait and Tulika Seth; BT/PR22985 from the Department of Biotechnology, Govt. of India to Prasenjit Guchhait, Sankar Bhattacharyya and Naval K. Vikram; and Tata Innovation Fellowship BT/HRD/35/01/02/2014 from the Department of Biotechnology, Govt. of India to Anirban Basu

(NBRC). None of the above funders had any role in study design, data collection, data analysis, interpretation, writing of the report.

Acknowledgements

The authors thank Dr. Nirpendra Singh of Regional Centre for Biotechnology for helping in proteomic data analysis, and to Dr. Bibhabasu Hazra of NBRC for useful suggestions in signaling related work. Authors sincerely acknowledge Dr. Priya Kalra of All India Institute of Medical Sciences, New Delhi for carefully reading and editing the manuscript.

References

- Assinger A, Kral JB, Yaiw KC, et al. Human cytomegalovirus-platelet interaction triggers toll-like receptor 2-dependent proinflammatory and proangiogenic responses. *Arterioscler Thromb Vasc Biol* 2014;34(4):801–9.
- Afdhal N, McHutchison J, Brown R, et al. Thrombocytopenia associated with chronic liver disease. *J Hepatol* 2008;48(6):1000–7.
- Chaipan C, Soilleux EJ, Simpson P, et al. DC-SIGN and CLEC-2 mediate human immunodeficiency virus type 1 capture by platelets. *J Virol* 2006;80(18):8951–60.
- Geisbert TW, Hensley LE, Jahrling PB, et al. Treatment of Ebola virus infection with a recombinant inhibitor of factor VIIa/tissue factor: a study in rhesus monkeys. *Lancet* 2003;362(9400):1953–8.
- Ojha A, Nandi D, Batra H, et al. Platelet activation determines the severity of thrombocytopenia in dengue infection. *Sci Rep* 2017;7:41697.
- Simon AY, Sutherland MR, Prydzial EL. Dengue virus binding and replication by platelets. *Blood* 2015;126(3):378–85.
- Weksler BB. Review article: the pathophysiology of thrombocytopenia in hepatitis C virus infection and chronic liver disease. *Aliment Pharmacol Ther* 2007;26(Suppl. 1):13–9.
- Bouwman JJ, Visseren FL, Bosch MC, Bouter KP, Diepersloot RJ. Procoagulant and inflammatory response of virus-infected monocytes. *Eur J Clin Invest* 2002;32(10):759–66.
- Zapata JC, Cox D, Salvato MS. The role of platelets in the pathogenesis of viral hemorrhagic fevers. *PLoS Negl Trop Dis* 2014;8(6):e2858.
- Malavige GN, Wijewickrama A, Fernando S, et al. A preliminary study on efficacy of rupatadine for the treatment of acute dengue infection. *Sci Rep* 2018;8(1):3857.
- Trugilho MRO, Hottz ED, Brunoro GVF, et al. Platelet proteome reveals novel pathways of platelet activation and platelet-mediated immunoregulation in dengue. *PLoS Pathog* 2017;13(5):e1006385.
- Auerbach DJ, Lin Y, Miao H, et al. Identification of the platelet-derived chemokine CXCL4/PF-4 as a broad-spectrum HIV-1 inhibitor. *Proc Natl Acad Sci U S A* 2012;109(24):9569–74.
- Schwartzkopff F, Grimm TA, Lankford CS, et al. Platelet factor 4 (CXCL4) facilitates human macrophage infection with HIV-1 and potentiates virus replication. *Innate Immun* 2009;15(6):368–79.
- Zaldivar MM, Pauels K, von Hundelshausen P, et al. CXC chemokine ligand 4 (Cxc4) is a platelet-derived mediator of experimental liver fibrosis. *Hepatology* 2010;51(4):1345–53.
- Guo L, Feng K, Wang YC, et al. Critical role of CXCL4 in the lung pathogenesis of influenza (H1N1) respiratory infection. *Mucosal Immunol* 2017;10(6):1529–41.
- Cocchi F, Devico AL, Garzino-Demo A, Arya SK, Gallo RC, Lusso P. Identification of RANTES, MIP-1 alpha, and MIP-1 beta as the major HIV-suppressive factors produced by CD8+ T cells. *Science* 1995;270(5243):1811–5.
- Wareing MD, Lyon AB, Lu B, Gerard C, Sarawar SR. Chemokine expression during the development and resolution of a pulmonary leukocyte response to influenza A virus infection in mice. *J Leukoc Biol* 2004;76(4):886–95.
- Katsounas A, Schlaak JF, Lempicki RA. CCL5: a double-edged sword in host defense against the hepatitis C virus. *Int Rev Immunol* 2011;30(5–6):366–78.
- Wilson SS, Wiens ME, Smith JG. Antiviral mechanisms of human defensins. *J Mol Biol* 2013;425(24):4965–80.
- Mohan KV, Rao SS, Atreya CD. Antiviral activity of selected antimicrobial peptides against vaccinia virus. *Antiviral Res* 2010;86(3):306–11.
- Lang PA, Contaldo C, Georgiev P, et al. Aggravation of viral hepatitis by platelet-derived serotonin. *Nat Med* 2008;14(7):756–61.
- Koupenova M, Vitseva O, MacKay CR, et al. Platelet-TLR7 mediates host survival and platelet count during viral infection in the absence of platelet-dependent thrombosis. *Blood* 2014;124(5):791–802.
- Othman M, Labelle A, Mazzetti I, Elbatarny HS, Lillcrap D. Adenovirus-induced thrombocytopenia: the role of von Willebrand factor and P-selectin in mediating accelerated platelet clearance. *Blood* 2007;109(7):2832–9.
- Littau R, Kurane I, Ennis FA. Human IgG Fc receptor II mediates antibody-dependent enhancement of dengue virus infection. *J Immunol* 1990;144(8):3183–6.
- Rodenhuis-Zybert IA, Wilschut J, Smit JM. Dengue virus life cycle: viral and host factors modulating infectivity. *Cell Mol Life Sci* 2010;67(16):2773–86.
- Durbin AP, Vargas MJ, Wanionek K, et al. Phenotyping of peripheral blood mononuclear cells during acute dengue illness demonstrates infection and increased activation of monocytes in severe cases compared to classic dengue fever. *Virology* 2008;376(2):429–35.
- Peschke T, Bender A, Nain M, Gerns D. Role of macrophage cytokines in influenza A virus infections. *Immunobiology* 1993;189(3–4):340–55.
- Baron S, Dianzani F. The interferons: a biological system with therapeutic potential in viral infections. *Antiviral Res* 1994;24(2–3):97–110.
- Dianzani F. Interferon treatments: how to use an endogenous system as a therapeutic agent. *J Interferon Res* 1992:109–18.
- Singhal R, Chawla S, Batra H, et al. Engulfment of Hb-activated platelets differentiates monocytes into pro-inflammatory macrophages in PNH patients. *Eur J Immunol* 2018;48(8):1285–94.
- Singhal R, Annarapu GK, Pandey A, et al. Hemoglobin interaction with GP1balpha induces platelet activation and apoptosis: a novel mechanism associated with intravascular hemolysis. *Haematologica* 2015;100(12):1526–33.
- Mukherjee S, Singh N, Sengupta N, et al. Japanese encephalitis virus induces human neural stem/progenitor cell death by elevating GRP78, PHB and hnRNPc through ER stress. *Cell Death Dis* 2017;8(1):e2556.
- Waugh MG, Chu KM, Clayton EL, Minogue S, Hsuan JJ. Detergent-free isolation and characterization of cholesterol-rich membrane domains from trans-Golgi network vesicles. *J Lipid Res* 2011;52(3):582–9.
- Suriyanarayanan T, Qingsong L, Kwang LT, Mun LY, Truong T, Seneviratne CJ. Quantitative Proteomics of strong and Weak Biofilm Formers of *Enterococcus faecalis* reveals Novel regulators of Biofilm Formation. *Mol Cell Proteomics* 2018;17(4):643–54.
- Vaudel M, Barsnes H, Berven FS, Sickmann A, Martens L. SearchGUI: an open-source graphical user interface for simultaneous OMSSA and X!Tandem searches. *Proteomics* 2011;11(5):996–9.
- Elias JE, Gygi SP. Target-decoy search strategy for mass spectrometry-based proteomics. *Methods Mol Biol* 2010;604:55–71.
- Apweiler R, Bairoch A, Wu CH, et al. UniProt: the universal protein knowledgebase. *Nucleic Acids Res* 2004;32(Database issue):D115–9.
- Zybailov B, Mosley AL, Sardiou ME, Coleman MK, Florens L, Washburn MP. Statistical analysis of membrane proteome expression changes in *Saccharomyces cerevisiae*. *J Proteome Res* 2006;5(9):2339–47.
- Vaudel M, Burkhart JM, Zahedi RP, et al. PeptideShaker enables reanalysis of MS-derived proteomics data sets. *Nat Biotechnol* 2015;33(1):22–4.
- Powell DW, Weaver CM, Jennings JL, et al. Cluster analysis of mass spectrometry data reveals a novel component of SAGA. *Mol Cell Biol* 2004;24(16):7249–59.
- Eslin DE, Zhang C, Samuels KJ, et al. Transgenic mice studies demonstrate a role for platelet factor 4 in thrombosis: dissociation between anticoagulant and antithrombotic effect of heparin. *Blood* 2004;104(10):3173–80.
- Brandt E, Ernst M, Loppnow H, Flad HD. Characterization of a platelet derived factor modulating phagocyte functions and cooperating with interleukin 1. *Lymphokine Res* 1989;8(3):281–7.
- Deuel TF, Senior RM, Chang D, Griffin GL, Heinrichson RL, Kaiser ET. Platelet factor 4 is chemotactic for neutrophils and monocytes. *Proc Natl Acad Sci U S A* 1981;78(7):4584–7.
- Parker ZF, Rux AH, Riblett AM, et al. Platelet factor 4 Inhibits and Enhances HIV-1 Infection in a Concentration-Dependent Manner by Modulating Viral Attachment. *AIDS Res Hum Retroviruses* 2016;32(7):705–17.
- Rhodes GR, Dixon RH, Silver D. Heparin induced thrombocytopenia with thrombotic and hemorrhagic manifestations. *Surg Gynecol Obstet* 1973;136(3):409–16.
- Mishra MK, Basu A. Minocycline neuroprotects, reduces microglial activation, inhibits caspase 3 induction, and viral replication following Japanese encephalitis. *J Neurochem* 2008;105(5):1582–95.
- Zompi S, Harris E. Animal models of dengue virus infection. *Viruses* 2012;4(1):62–82.
- Ha Y, Liu H, Zhu S, et al. Critical Role of the CXCL10/C-X-C Chemokine Receptor 3 Axis in Promoting Leukocyte Recruitment and Neuronal Injury during Traumatic Optic Neuropathy Induced by Optic Nerve Crush. *Am J Pathol* 2017;187(2):352–65.
- Zhang X, Han J, Man K, et al. CXC chemokine receptor 3 promotes steatohepatitis in mice through mediating inflammatory cytokines, macrophages and autophagy. *J Hepatol* 2016;64(1):160–70.
- Walser TC, Rifat S, Ma X, et al. Antagonism of CXCR3 inhibits lung metastasis in a murine model of metastatic breast cancer. *Cancer Res* 2006;66(15):7701–7.